SWT Report No. 81-3

LEVEL II 2

AFOSR TR_____

THE COMPRESSIBLE LAMINAR TWO-DIMENSIONAL WAKE WITH ARBRITRARY INITIAL ASYMMETRY

Prepared by
Anthony Demetriades

for

Air Force Office of Scientific Research
Building 410
Bolling Air Force Base
Washington D.C. 20332
under Grant AFOSR 80-0267

Supersonic Wind-Tunnel Laboratory
Department of Mechanical Engineering
Montana State University
Bozeman, Montana 59717

July 1981

Unclassified
SECURITY CLASSIFICATION OF THIS PAGE (When Data Entered)

REPORT DOCUMENTATION PAGE	READ INSTRUCTIONS BEFORE COMPLETING FORM
1. REPORT NUMBER: AFOSR-TR- 81 -0841 / 2. GOVT ACCESSION NO.: AD-A109084	3. RECIPIENT'S CATALOG NUMBER:
4. TITLE (and Subtitle): The Compressible Laminar Two-Dimensional Wake With Arbritrary Initial Asymmetry	5. TYPE OF REPORT & PERIOD COVERED: (ANNUAL) 1 October 1980 - 30 Sept. 8
	6. PERFORMING ORG. REPORT NUMBER: SWT Report No. 81-3
7. AUTHOR(s): Anthony Demetriades	8. CONTRACT OR GRANT NUMBER(s): AFOSR 80-0267
9. PERFORMING ORGANIZATION NAME AND ADDRESS: Mechanical Engineering Department, Montana State University, Bozeman, MT 59717	10. PROGRAM ELEMENT, PROJECT, TASK AREA & WORK UNIT NUMBERS: 61102F, 2307/A2
11. CONTROLLING OFFICE NAME AND ADDRESS: Air Force Office of Scientific Research/NA, Building 410, Bolling AFB, DC 20332	12. REPORT DATE: July 1981
	13. NUMBER OF PAGES: 76
14. MONITORING AGENCY NAME & ADDRESS (if different from Controlling Office)	15. SECURITY CLASS. (of this report): UNCLASSIFIED
	15a. DECLASSIFICATION DOWNGRADING SCHEDULE

16. DISTRIBUTION STATEMENT (of this Report)

Approved for public release; distribution unlimited

17. DISTRIBUTION STATEMENT (of the abstract entered in Block 20, if different from Report)

18. SUPPLEMENTARY NOTES

19. KEY WORDS (Continue on reverse side if necessary and identify by block number)

Laminar flow, wakes, free shear flows

20. ABSTRACT (Continue on reverse side if necessary and identify by block number)

Closed-form analytic solutions are presented for the two-dimensional laminar wake, which are applicable from the trailing edge to infinte downstream distances, and for any "initial asymmetry" ratio of the two merging boundary layer thicknesses. An initially exponential velocity profile is assumed, and Goldstein's treatment is utilized of the evolution of the profile based on the Oseen approximation. The solutions show the effect of edge Mach number, Reynolds number, wall-to-stagnation temperature ratio and asymmetry factor. Beyond a certain distance from the

DD FORM 1 JAN 73 1473

UNCLASSIFIED

SECURITY CLASSIFICATION OF THIS PAGE (When Data Entered)

trailing edge the solutions reduce to the well-known asymptotic behavior regardless of the magnitude of these parameters. In the "non-equilibrium" region from the trailing edge to the equilibration distance, the supersonic/hypersonic cooled wake behaves rather abnormally. The effect of initial asymmetry is to deflect the wake center off the plane of the trailing edge, and to displace the wake "center" of the velocity relative to the temperature-density center without much affecting the velocity, temperature or density defect magnitudes or the wake thickness. Comparison with earlier work shows very good agreement with the Tollmien-Goldstein implicit solutions near the trailing edge for symmetric incompressible flows. Good agreement is also found with available experimental data.

FOREWORD

This work was performed at the Supersonic Wind-Tunnel Laboratory of Montana State University by A. Demetriades, Professor Mechanical Engineering, under Grant AFOSR 80-0267 with the Air Force Office of Scientific Research of Washington D.C. It is part of a series of theoretical and experimental studies of the high-speed mixing characteristics of laminar, transitional, and turbulent shear flows.

In a practical sense, this study furnishes theoretical predictions of wake flows needed to optimize gas-dynamic and chemical laser design. As such, it was most recently motivated by work done by the author for the Air Force Weapons Laboratory and TETRA Corporation of Albuquerque, New Mexico. Specifically, the present problem was first discussed in TETRA report TR-81-005 by the present author, in which the solutions for the velocity were first shown. In the present report, the subject is continued by presenting the solutions for the thermodynamic variables as well. For the sake of completeness, the earlier velocity-field solutions are also briefly discussed.

A second, related motivation arises from the need to prepare theoretical predictions for certain experiments planned in the laboratory's supersonic tunnel for the AFOSR program. These experiments feature the basic fluid mechanics of asymmetric wakes and shear layers at supersonic speeds, for which predictive formulas are presented here. Clearly, if the latter are verified by the forthcoming experiments, the present analysis can become an important tool in laser cavity design.

Encouragement of, and interest in this work, has therefore come from diverse sources which the author wishes to acknowledge here. The assistance and cooperation of Drs. W. Moeny of TETRA and P. J. Ortwerth and L. Wilson of AFWL, as well as of Capt. M. Francis of AFOSR is noted with gratitude.

TABLE OF CONTENTS

LIST OF SYMBOLS

b^* : physical wake half-thickness

B : a constant function of M_e, T_w/T_o (eq. (29))

C : a constant (eq. (30))

F : non-dimensional lateral similarity coordinate (eq. (50))

F_c : value of F at wake center

$\bar{h}$: $\frac{T}{T_e} - 1$ (temperature function)

$\bar{h}_o$: value of $\bar{h}$ at the T.E.

H : total temperature defect (eq. (64))

$\bar{H}$: total temperature decrement (eq. (65))

$\tilde{H}$: total temperature profile (eq. (66))

G : integration kernel (eq. (9))

k : modulus in initial profile exponent

ℓ : length of hypothetical plate generating wake

L : scale length

M : Mach number

P : asymmetry ratio θ_1/θ_2

r : density defect (eq. (59))

$\bar{r}$: density decrement eq. (60))

Re' : unit Reynolds number = $\frac{u_e}{\nu_e}$

Re : Reynolds number

Re_L : Reynolds number based on $L = \frac{u_e L}{\nu_e}$

Re_θ : Reynolds number based on Momentum thickness θ

Re_Θ : Reynolds number based on $\Theta = \theta_1 + \theta_2$, $Re_\Theta \equiv \frac{u_e \Theta}{\nu_e}$

t : temperature defect (eq. (51))

t' : temperature decrement (eq. (55))

T : temperature

T_o : total temperature (used for variable local total temperature as well as for fixed flow stagnation temperature).

$\tilde{T}$: temperature profile (eq. (56))

T.E.: Trailing edge (origin of x, x')

u : flow velocity

$\bar{u}$: $1 - \frac{u}{u_e}$

$\bar{u}_o$: initial value of $\bar{u}$

$\tilde{u}$: velocity profile, eq. (45)

w : velocity defect, eq. (44) or (74)

x^* : longitudinal coordinate (dimensional)

x : non-dimensional longitudinal coordinate, eq. (25)

x' : non-dimensional longitudinal coordinate eq. (36)

y^* : lateral coordinate (dimensional, physical)

$\tilde{y}$: compressible-transformed lateral coordinate eq. (7)

y : non-dimensional lateral coordinate, eq. (26)

y' : non-dimensional lateral coordinate, eq. (37)

y'_{cu}: velocity center position of asymmetric wake

y'_{cT}: temperature center position of asymmetric wake

y'_{c} : density center position of asymmetric wake

δ : kinematic boundary-layer thickness

θ : momentum thickness

Θ : total momentum thickness $\theta_1 + \theta_2$

μ : viscosity

ν : kinematic viscosity

η_0 : lateral coordinate, same as y but at x = o

ρ : density

$\tilde{\rho}$: density profile, eq. (61)

σ : Prandtl number

$(\ )_1$: quantity in y > 0 half-plane

$(\ )_2$: quantity in y < 0 half-plane

$(\cdot)^*$: physical, dimensional property

$(\ )_e$: edge or free stream property

$(\ )_c$: quantity at wake center

$(\ )(0)$: quantity on y = 0 plane

$(\ )_w$: wall property

$(\ )_o$: property at x = 0 (except T_o)

LIST OF ILLUSTRATIONS

1. Introduction

The problem addressed in this report is the steady, laminar two-dimensional wake formed by a homogeneous fluid streaming past an infinitely thin plate. As enunciated, this problem was first solved for incompressible flow by Tollmien (Reference 1) and Goldstein (Reference 2). These solutions take a simple self-similar form far away from the trailing edge (T.E.), which has also been used as a convenient starting point in the discussion of compressible wakes (Reference 3). In the region immediately past the T.E. the classic solutions of References 1 and 2, however, have been arrived at in the form of matching expansions, which produces tabulated numerical results rather than a single analytic expression. It would clearly be desireable to have closed-form analytic solutions instead, in a way improving the perception of the wake behavior.

This report sets out to accomplish two objectives, the first of which is the derivation of formulas for the wake properties which are valid from the T.E. to an infinite distance downstream. This is done at any stream Mach and Reynolds numbers and any T.E. surface temperature relative to the stagnation temperature, by restricting the analysis to isobaric flow, Prandtl number one and constant Chapman-Rubesin factor. These restrictions are certainly not severe enough to obscure the dynamics, and can be removed once the basic problem is understood.

The second objective is to extend the solutions to a wake with initial asymmetry. In reallistic terms, such an asymmetry is more likely to occur, say, when two adjacent nozzles discharge parallel streams, as shown on Figure 1, than in the classic flat-plate wake. In fact, the motivation for this work arose from questions of gas-dynamic and chemical laser design optimization, which deal with geometries such as that of Figure 1. Since the two streams are identical, the asymmetry can arise only due to surface conditions at the T.E., such as different momentum thicknesses or different wall temperatures on either side of the T.E. The latter is rather unreallistic, however, so long as we consider the partition near the T.E as "infinitely thin". Thus, we consider only the asymmetry due to momentum-thickness differences in the two merging boundary layers.

It must be noted that the method of solution for both the symmetric and asymmetric cases rests on a linearization assumption. However, since the initial and asymptotic conditions at large distances are recovered, the penalty for this assumption is nowhere evident.

2. Statement of the Problem and Definition of Terms

The solution of the wake problem given herein is subject to the following restrictions:

1) The flow is everywhere parallel and two-dimensional.
2) The pressure is everywhere constant.
3) The fluid is chemically homogeneous and non-reacting.
4) No volume effects (e.g. volume heat addition or body force) are allowed.
5) The flow is laminar and steady.

A lesser assumption is that the Prandtl number is unity everywhere, chosen consistently with the use of the Crocco relation for the temperature distribution in the boundary layer at the trailing edge (T.E.).

Within these restrictions, the solutions are provided for:

(a) Any stream Mach number M_e.
(b) Any Reynolds number Re.
(c) Any wall-to-stagnation temperature ratio T_w/T_o (T_w is the T.E. surface temperature).
(d) Any asymmetry ratio $\theta_1/\theta_2 = P$.

The solutions are thus provided as functions of x, y, M, T_w/T_o, P and Re, the latter implicitly through the definition of the non-dimensional variables. When $\theta_1 = \theta_2$ or P = 1, the solution is termed <u>symmetric</u>, whereas the term "completely asymmetric" denotes the solution for P = 0 (or P = ∞).

The terms defect, deficit, and decrement are used to denote characteristic groupings of the flow variables at a certain x from the T.E. For example, for the temperature:

$$T(0) - T_e \text{ or } T_c - T_e : \text{deficit}$$

$$\frac{T(0) - T_e}{T_e} \quad \text{or} \quad \frac{T_c - T_e}{T_e} : \text{defect}$$

$$\frac{T(0) - T_e}{T_w - T_e} \quad \text{or} \quad \frac{T_c - T_e}{T_w - T_e} : \text{decrement}$$

The subscript "c" (for "center") is used to denote the extremum of the temperature profile at a certain x for the general case of wake asymmetry ($P \neq 1$). When $P = 1$, T_c coincides with $T(0)$, the latter symbolism meaning the temperature at $y = 0$ which is also the wake "center" (plane of symmetry) when $P = 1$.

The term "profile" is reserved for specific non-dimensional groupings such as

$$\frac{u_e - u}{u_e - u(0)} \quad \text{or} \quad \frac{u_e - u}{u_e - u_c}$$

while the term "variation" is often used to represent groupings such as $1 - u/u_e$.

3. Solution of the Problem for Arbritrary Asymmetry

3.1 The Method of Solution

The present objective is to find the fluid properties (velocity, temperature, density, etc.) in the wake as a function of the coordinates, the flow parameters, and the asymmetry ratio P. To this end, we utilize the solution reported by Gold (Reference 4) for a wake beginning at the T.E. with profiles

$$\bar{u}(x^*, y^*) \equiv 1 - \frac{u(x^*, y^*)}{u_e} \qquad (1)$$

$$\bar{h}(x^*, y^*) \equiv \frac{T(x^*, y^*)}{T_e} - 1 \tag{2}$$

of the velocity and temperature. Gold employed the Oseen approximation to the boundary-layer equations to find the solutions as follows:

$$\bar{u}(x,y) = \frac{1}{2\sqrt{x}} \int_{-\infty}^{\infty} \bar{u}_o(\xi)\, G(\xi; x, y)\, d\xi \tag{3}$$

$$\bar{h}(x,y) = \frac{1}{2\sqrt{x}} \int_{-\infty}^{\infty} \bar{h}_o(\xi)\, G(\xi; x, y)\, d\xi \tag{4}$$

where $\bar{u}_o$, $\bar{h}_o$: initial velocity and temperature profiles, and

$$x \equiv \frac{x^*}{L} \tag{5}$$

$$y \equiv \frac{\tilde{y}}{L}\sqrt{Re_L} \tag{6}$$

$$\tilde{y} \equiv \int_0^y \frac{\rho^*}{\rho_e}\, dy^* \tag{7}$$

L = characteristic length, to be derived.

$$Re_L \equiv \frac{u_e L}{\nu_e} \tag{8}$$

$$G(\xi; x, y) = \frac{1}{\sqrt{\pi x}} \exp\left[-(y-\xi)^2/4x\right] \tag{9}$$

The Oseen approximation is a linearization restricted to:

$$\bar{u} << 1 \tag{10}$$

$$\bar{h} << 1 \tag{11}$$

Note that dimensional properties above, are usually denoted by an asterisk (*) or a subscript "e".

Three additional remarks must be made as regards the above solution. First, Gold assumed the Chapman-Rubesin factor $\mu\rho$ as constant; second, the coordinate x appearing in eq. (5) was written by Gold as x/σ, to account for non-unity Prandtl number. Here we set $\sigma = 1$ to be consistent with our later use of the Crocco relation. This difference can be easily accounted for in numerical calculations, and is in anyway a rather unimportant feature of this analysis.

Third, Gold calculated that the solutions (3) and (4) are rather insensitive to the initial profiles $\bar{u}_o$ and $\bar{h}_o$ especially far from the origin, and that the governing factor is the initial momentum thickness rather than the initial profile shape. This should be kept in mind in the next section.

3.2 The Initial Profiles

If the shed boundary layers have momentum thicknesses θ_1 and θ_2 respectively, then the initial velocity profile at the T.E. for purposes of calculating the wake development is:

$$\text{For} \quad y^*, \tilde{y} > 0 \quad : \quad \bar{u}_o \equiv 1 - \frac{u_o}{u_e} = e^{-k_1 \tilde{y}} \tag{12}$$

$$y^*, \tilde{y} < 0 \quad : \quad e^{k_2 \tilde{y}} \tag{13}$$

with k_1, k_2 evaluated from the linearized version

$$\theta \simeq \int_0^\infty \bar{u}_o \, dy^* \tag{14}$$

of the momentum integral

$$\theta = \int_0^\infty \frac{\rho}{\rho_e} \frac{u}{u_e} \left(1 - \frac{u}{u_e}\right) dy^* = \int_0^\infty \frac{u}{u_e} \left(1 - \frac{u}{u_e}\right) d\tilde{y} = \int_0^\infty \bar{u}_o (1 - \bar{u}_o) \, d\tilde{y} \tag{15}$$

where

$$\tilde{y} = \int_0^{y^*} \frac{\rho}{\rho_e} \, dy^* \tag{16}$$

Use of (14) instead of (15) as a boundary condition is consistent with Gold's theory which is used past the T.E. and it implies that

$$w \equiv 1 - \frac{u(o)}{u_e} << 1 \tag{17}$$

Using (12), (13) in (14) gives

$$k_1 = \theta_1, \; k_2 = \theta_2 \tag{18}$$

so that the initial velocity profile reads

$$\tilde{y} > o : \bar{u}_o = e^{-\tilde{y}/\theta_1} = e^{-y} \tag{19}$$

$$\tilde{y} < o : \bar{u}_o = e^{\tilde{y}/\theta_2} = e^{Py} \tag{20}$$

with

$$y \equiv \tilde{y}/\theta_1 \tag{21}$$

$$P \equiv \theta_1/\theta_2 \tag{22}$$

The choice for an exponential initial velocity profile is arbritrary, although it has obvious qualitative similarities to a "typical" profile as Figure 2 shows; clearly, too, it is algebraically simple and should therefore expedite the solution. The earlier comments should also be recalled, regarding the insignificance of the initial profile details to the wake development. It is more important to note that the chosen profiles (19) and (20) cannot possibly fulfill the condition (10). We shall see from the results that the solution is analytic for all $x > 0$, however, and that a very reasonable continuous solution is obtained.

The parameter P, called the asymmetry ratio, is a key parameter in this analysis because it shows the initial "skewness" of the wake. Because of the interchangeability of θ_1 and θ_2 the range $0 < P < 1$ covers all possible ratios of θ_1 and θ_2.

For consistency, the definition of y must be carried from the T.E. to all downstream positions. This allows us to define the length scale L by combining (6) and (21):

$$\frac{\tilde{y}}{L}\sqrt{Re_L} = \frac{\tilde{y}}{\theta_1} \tag{23}$$

$$L = \theta_1 Re_{\theta_1}\ ,\quad Re_{\theta_1} = \frac{u_e}{\nu_e}\theta_1 \tag{24}$$

so that the non-dimensional variables x and y in the proposed solution (3) become, according to (23) and (24):

$$x \equiv \frac{x^*}{\theta_1 Re_{\theta_1}} \tag{25}$$

$$y \equiv \frac{\tilde{y}}{\theta_1} \tag{26}$$

We perceive that the choice of L can be further improved, to avoid awkward mathematics such as for P = 0 ($\theta_1 = 0$). Besides, it should be clear that the wake should be controlled by its total drag, i.e. θ_1 and θ_2, and by P which shows how this drag was initially distributed between streams 1 and 2. We will make this improvement on L later, since it is more convenient to first present the solution in terms of the coordinates as defined by (25) and (26).

The initial temperature profiles were found with the aid of the Crocco relation:

$$\frac{T}{T_e} = \frac{T_w}{T_e} + \left(1 + \frac{\gamma-1}{2}M_e^2 - \frac{T_w}{T_e}\right)\frac{u}{u_e} - \frac{\gamma-1}{2}M_e^2\left(\frac{u}{u_e}\right)^2 \tag{27}$$

Using the definitions

$$\bar{h}_0 \equiv \left(\frac{T}{T_e} - 1\right)_{x=0} \tag{28}$$

$$B \equiv \frac{\gamma-1}{2}M_e^2 - 1 + \frac{T_w}{T_e} \tag{29}$$

$$C \equiv -\frac{\gamma-1}{2}M_e^2 \tag{30}$$

as well as equations (19) and (20) we obtain

$$y > 0 : \quad \bar{h}_0 = B e^{-y} + C e^{-2y} \tag{31}$$

$$y < 0 : \quad \bar{h}_0 = B e^{Py} + C e^{2Py} \tag{32}$$

The Crocco relation (28) is valid when the Prandtl number $\sigma = 1$. For this reason, as already mentioned, consistency requires that the wake solutions are found for $\sigma = 1$ also, as we intend to do.

Typical initial temperature profiles according to (31) and (32), are illustrated on Figure 3, and are useful in stressing two points. First, the examples of Figure 3 were chosen to illustrate the possibility that for certain M_e and T_w/T_0 we can obtain $\bar{h}_0 > > 1$, which violates the assumption (11). This violation is more serious than in the case of the velocity where $\bar{u}_0 = 1$ at most; thus the temperature results of the present analysis should be viewed with caution near $x = 0$. Second, the distribution of temperature is plotted in two different ways, the "profile" function being shown on the right of the Figure. The algebraic form of the profile often creates unusual curves, a point to be kept in mind during the presentation of results.

3.3 Solutions

If the initial profiles (19), (20), (31) and (32) are substituted in eq. (30) and (4), simple, closed-form solutions can be immediately obtained for $\bar{u}$ and :

$$\bar{u}(x,y;P) = \frac{1}{2}\left[e^{P^2x+Py}\left(1-Erf\sqrt{x}\left(P+\frac{y}{2x}\right)\right) + e^{x-y}\left(1+Erf\sqrt{x}\left(\frac{y}{2x}-1\right)\right)\right] \tag{33}$$

$$\bar{h}(x,y;P,M_e,\tfrac{T_w}{T_0}) = \frac{1}{2}\left[B\left[e^{x-y}\left(1-Erf\sqrt{x}\left(1-\frac{y}{2x}\right)\right)+e^{xP^2+Py}\left(1-\right.\right.\right. \tag{34}$$

$$\left.\left.\left.-Erf\sqrt{x}\left(P+\frac{y}{2x}\right)\right)\right]+C\left[e^{4x-2y}\left(1-Erf\sqrt{x}\left(2-\frac{y}{2x}\right)\right)+e^{4P^2x+2Py}\left(1-Erf\sqrt{x}\left(2P+\frac{y}{2x}\right)\right)\right]\right]$$

As expected, $\bar{u}$ does not explicitly depend on M_e and T_w/T_0, although it does so implicitly through the transformed variable $\tilde{y}$.

The solutions (33) and (34) have been successfully subjected to the following tests:

(a) At $x = 0$, the initial profiles (19) etc. are recovered.

(b) At $y = \pm\infty$, $\bar{u} = \bar{k} = 0$ as expected.

(c) At $x = \infty$, the familiar Tollmien-Goldstein asymptotic forms are recovered as expected, independent of P. (References 1 and 2) The Tollmien-Goldstein asymptotes will be presented later.

(d) If θ_1 and θ_2 are interchanged relative to the positive sense of y, then the asymmetric solutions ($P \neq 1$) also interchange, as they should.

Solutions (33) and (34) are sufficient to determine the entire flow field since the pressure is constant; thus the density, Mach number, etc. can be determined directly.

Before anplying the solutions to special cases, it is here appropriate to change the independent variables into a more meaningful form. The total momentum thickness of the wake is

$$\Theta \equiv \theta_1 + \theta_2 \tag{35}$$

and it appears suitable to use Θ in place of θ_1 in the definitions of x and y (see (25) and (26)). The new variables therefore, are:

$$x' \equiv \frac{x^*}{\Theta Re_\Theta} = \frac{x^*}{\Theta^2 Re'} \tag{36}$$

$$y' \equiv \frac{\tilde{y}}{\Theta} \tag{37}$$

The connection between x, y, and x', y' can be found using (35):

$$x = \frac{(P+1)^2}{P^2} x' \tag{38}$$

and

$$y = \frac{P+1}{P} y' \tag{39}$$

The solutions (33) and (34) thus become:

$$\bar{u} = \frac{1}{2}\left[e^{(P+1)^2x' + (P+1)y'}\left(1 - \mathrm{Erf}\left((P+1)\sqrt{x'} + \frac{y'}{2\sqrt{x'}}\right)\right)\right.$$
$$\left. + e^{\left(\frac{P+1}{P}\right)^2 x' - \frac{P+1}{P}y'}\left(1 + \mathrm{Erf}\left(\frac{y'}{2\sqrt{x'}} - \frac{P+1}{P}\sqrt{x'}\right)\right)\right] \tag{40}$$

and

$$\bar{h} = \frac{1}{2}\left\{B\left[e^{\left(\frac{P+1}{P}\right)^2 x' - \frac{P+1}{P}y'}\left(1 - \mathrm{Erf}\left(\frac{P+1}{P}\sqrt{x'} - \frac{y'}{2\sqrt{x'}}\right)\right)\right.\right.$$
$$\left. + e^{(P+1)^2x' + (P+1)y'}\left(1 - \mathrm{Erf}\left((P+1)\sqrt{x'} + \frac{y'}{2\sqrt{x'}}\right)\right)\right] + C\left[e^{4x'\left(\frac{P+1}{P}\right)^2 - 2\left(\frac{P+1}{P}\right)y'}\right.$$
$$\left.\left.\left(1 - \mathrm{Erf}\left(2\sqrt{x'}\frac{P+1}{P} - \frac{y'}{2\sqrt{x'}}\right)\right) + e^{4(P+1)^2x' + 2(P+1)y'}\left(1 - \mathrm{Erf}\left(2(P+1)\sqrt{x'} + \frac{y'}{2\sqrt{x'}}\right)\right)\right]\right\} \tag{41}$$

It should be parenthetically noted that the variable $y'/2\sqrt{x'}$ is insensitive to the choice of the normalizing length, as can be seen by inspection of eqs. (36) and (37).

4. The Symmetric Wake

As mentioned in the Introduction, a complete analytic solution from the T.E. downstream has not yet been reported for the symmetric two-dimensional wake, regardless of M or T_w/T_0. Such a solution can be obtained directly from (40) and (41) by setting P = 1. Then,

$$\bar{u} = \frac{1}{2}\left[e^{4x'+2y'}\left(1 - \mathrm{Erf}\left(\frac{y'}{2\sqrt{x'}} + 2\sqrt{x'}\right)\right) + e^{4x'-2y'}\left(1 + \mathrm{Erf}\left(\frac{y'}{2\sqrt{x'}} - 2\sqrt{x'}\right)\right)\right] \tag{42}$$

$$\bar{h} = \frac{1}{2}\left[B\left(e^{4x'-2y'}\left(1 - \mathrm{Erf}\left(2\sqrt{x'} - \frac{y'}{2\sqrt{x'}}\right)\right) + e^{4x'+2y'}\left(1 - \mathrm{Erf}\left(2\sqrt{x'} + \frac{y'}{2\sqrt{x'}}\right)\right)\right)\right.$$
$$\left. + C\left(e^{16x'-4y'}\left(1 - \mathrm{Erf}\left(4\sqrt{x'} - \frac{y'}{2\sqrt{x'}}\right)\right) + e^{16x'+4y'}\left(1 - \mathrm{Erf}\left(4\sqrt{x'} + \frac{y'}{2\sqrt{x'}}\right)\right)\right)\right] \tag{43}$$

These solutions are naturally symmetric in y'.

In the symmetric case, the wake center occurs at $y' = 0$, (i.e. the plane of symmetry) so that if the wake defect is defined as

$$W \equiv \frac{u_e - u(0)}{u_e} = \frac{u - u_c}{u_e} = W(x') \tag{44}$$

and the velocity profile as usual by

$$\tilde{u} \equiv \frac{u_e - u}{u_e - u(0)} = \tilde{u}(x', y') \tag{45}$$

then $$\bar{u} = w\tilde{u} \tag{46}$$

It can be easily shown from (42) that the defect is

$$w(x'; P=1) = e^{4x'}(1 - Erf\, 2\sqrt{x'}) \tag{47}$$

and that $W(x' = 0; P = 1) = 1$ as expected. At very large x', this defect becomes

$$w(x'=\infty; P=1) = \frac{1}{2\sqrt{\pi x'}} \tag{48}$$

which is well-known of the Tollmien (Ref. 1) and Goldstein (Ref. 2) and which has since been discussed by numerous authors (Ref. 3, 4).

The velocity profile begins, at $x' = 0$, with the double-cusp shape given by (19) and (20) and $P = 1$. The discontinuity at $y' = 0$ disappears just as soon as the fluid leaves the T.E.; for all $\tilde{x} > 0$ the $\tilde{u}$, found by combining (42), (46), and (47), is continuous and analytic in y'. At large x' it can be shown from (45) that

$$\tilde{u}(x'=\infty; P=1) = e^{-\frac{y'^2}{4x'}} \tag{49}$$

This simple result has been long known as the asymptotic form of the profile, which depends on the similarity variable

$$F \equiv \frac{y'}{2\sqrt{x'}} \tag{50}$$

The temperature distribution at the T.E. as given by (31) and (32) is of course generally discontinuous at $y = y' = 0$. Just like the velocity, this distribution develops a "rounded top" and is everywhere analytic immediately past the T.E. according to (43). On the plane of symmetry $y' = 0$, the temperature defect

$$t \equiv \bar{t}(0) \equiv \bar{t}\left(x', 0; P=1; Me, \frac{T_w}{T_0}\right) = \frac{T(0)}{T_e} - 1 =$$
$$= Be^{4x'}(1 - Erf\, 2\sqrt{x'}) + Ce^{16x'}(1 - Erf\, 4\sqrt{x'}) \tag{51}$$

At the trailing edge ($x' = 0$) the initial defect is

$$t(x'=0) = B + C = \frac{T_w}{T_e} - 1 \tag{52}$$

as also indicated by (31) and (32). Far from the T.E. on the other hand,

$$t(x'=\infty) = \bar{h}(\infty, 0; P=1; M_e, \frac{T_w}{T_0}) = \frac{1}{2\sqrt{\pi x'}}\left(B + \frac{C}{2}\right) \tag{53}$$

Combining with (47) we note that at large x' the ratio of the temperature to the velocity defects is a constant dependent on M_e and T_w/T_0 only:

$$\frac{t}{w} = B + \frac{C}{2} = \frac{\gamma-1}{2} M_e^2 \left(\frac{1}{2} + \frac{T_w}{T_0}\right) + \left(\frac{T_w}{T_0} - 1\right) \tag{54}$$

Here the first term on the r.h.s. indicates the compressibility effect on wake temperature, while the second term indicates the effect of the surface temperature only. There is, of course, a Prandtl number effect which is ignored here as per earlier comments; if the Prandtl number σ was included, then the entire r.h.s. of (54) would be multiplied by σ.

In addition to the temperature defect as defined in (51), we can consider the temperature decrement

$$t' \equiv \frac{T(0)-T_e}{T_w - T_e} = t'(x'; M_e, \frac{T_w}{T_0}) \tag{55}$$

which is always unity at the T.E. as opposed to the defect which can be larger than unity at $x' = 0$. The decrement, which is simply related to t via the ratio T_w/T_0, is useful when the latter is different from unity.

The temperature profile

$$\tilde{T} \equiv \frac{T-T_e}{T(0)-T_e} \tag{56}$$

is equal to the ratio $\bar{h}/t$ and can be thus found from (43) and (51). At the T.E., the profile is given for P = 1 by the initial conditions (31) and (32); at large x', on the other hand, the profile asymptotic form is again

$$\tilde{T}(x'=\infty) = e^{-y'^2/4x'} = e^{-F^2} = \tilde{u}(x'=\infty) \tag{57}$$

which is again a consequence of $\sigma = 1$. Parenthetically note that, in general,

$$\tilde{T}(x'=\infty, \sigma \neq 1) = e^{-\sigma F^2} \tag{58}$$

The fact that the asymptotic velocity and temperature profiles (49) and (57) agree with the long-known results of Tollmien and others is an important cross-check of the present analysis.

Other flow variables, such as the density, total temperature and Mach number, can be obtained in the above manner quite directly. For the sake of completeness, these variables will be given below.

Using its customary definition, the density defect is

$$\tau \equiv \frac{\rho_e - \rho(0)}{\rho_e} = \frac{t}{t+1} \tag{59}$$

with t given by (51). Similarly, the density decrement is

$$\bar{\tau} = \frac{\rho_e - \rho(0)}{\rho_e - \rho_w} = \tau\left(1 + \frac{1}{B+C}\right) \tag{60}$$

The density profile is

$$\tilde{\rho} \equiv \frac{\rho_e - \rho}{\rho_e - \rho(0)} = \tilde{T}\,\frac{t+1}{\tilde{T}t+1} \tag{61}$$

An inspection of these formulas for the density reveals once again that the density "lags" the fluid temperature in the attainment of similarity at large x'.

The local Mach number, M, in the wake is given by

$$M = M_e \frac{1-\tilde{u}w}{\sqrt{1+\tilde{T}t}} \tag{62}$$

and on the plane of symmetry ($\tilde{u}=\tilde{T}=1$):

$$M(0) = M_e \frac{1-w}{\sqrt{1+t}} \tag{63}$$

Finally, the total temperature defect

$$H \equiv \frac{T_0(0)}{T_{0e}} - 1 = (t+1)\,\frac{1+0.2\,M(0)^2}{1+0.2\,M_e^2} - 1 \qquad (\gamma=1.4) \tag{64}$$

while the total temperature decrement is

$$\bar{H} \equiv \frac{T_0(0) - T_{0e}}{T_w - T_{0e}} = \frac{H}{\frac{T_w}{T_0} - 1} \tag{65}$$

and the corresponding profile is

$$\tilde{H} \equiv \frac{T_o - T_{oe}}{T_o(0) - T_{oe}} = \frac{(1+\tilde{\tau}t)\,\frac{1+0.2M^2}{1+0.2M_\infty^2} - 1}{(1+t)\,\frac{1+0.2M(0)^2}{1+0.2M_\infty^2} - 1} \qquad (\gamma = 1.4) \tag{66}$$

Note that in the last few formulas, above, dealing with the local total temperature, the symbol for the latter is T_o. The quantity T_{oe} is the given total temperature of the stream, which in earlier sections was denoted by T_0.

Sample computations and plots for the symmetric wake will be presented in Section 6.

5. The Completely Asymmetric Wake

Early computations made in this work with eqs. (40) and (41) showed that considerable departures from the symmetric wake case given above, occur only for extreme values of the asymmetry ratio P, that is for $\theta_1 >> \theta_2$ or $\theta_1 << \theta_2$. It therefore seems reasonable to limit the analysis of wake asymmetry to the extreme case $\theta_1 = 0$ (P = 0) or $\theta_2 = 0$ (P = ∞). These two extreme cases are of course identical since one can be obtained from the other by mirror reflection of its flow field about the $y' = 0$ plane. We shall therefore discuss only the P = 0 case, which means that one of the two merging boundary layers is vanishingly small relative to the other. We call this the "completely asymmetric wake". (Of course, the general solutions (40) etc. can be used for arbritrary asymmetry).

For P = 0, the initial profiles at the T.E. are:

$$y' > 0: \qquad \bar{u}_o = 0 \tag{67}$$

$$y' < 0: \qquad \bar{u}_o = e^{\tilde{y}/\theta_2} = e^{\tilde{y}/\Theta} = e^{y'} \tag{68}$$

$$y' > 0: \qquad \bar{h}_o = 0 \tag{69}$$

$$y'<0: \bar{h}_0 = Be^{\frac{\tilde{y}}{\theta_2}} + Ce^{2\frac{\tilde{y}}{\theta_2}} = Be^{y'} + Ce^{2y'} \tag{70}$$

It is both necessary and intuitively possible, here, to preview the development of this asymmetric wake beyond the trailing edge. As x' increases, the above initial profiles will tend to "round off", but the "center of gravity" of the profile initially lies in the $y' < 0$ half space. It is therefore likely that the profile maximum (actual velocity minimum) will lie in $y' < 0$ and not $y' = 0$ as was the case of wake symmetry. This maximum will be referred to as the "wake center", and its path (the "deflection") away from $y' = 0$ is of some interest. For example, we can intuitively predict that the wake symmetrizes at large x', but not whether the center will return to the $y' = 0$ plane. The subscript "c" for "center" will in anyway assume the role the symbol (0) had for the symmetric case (see Section 2 also).

The solutions for the completely asymmetric wake can be directly obtained from (40) and (41) in the limit $P = 0$:

$$\bar{u}(x', y'; P=0) = \frac{1}{2}\left[e^{x'+y'}\left(1 - Erf\left(\sqrt{x'} + \frac{y'}{2\sqrt{x'}}\right)\right)\right] \tag{71}$$

$$\bar{h}(x', y'; P=0; M_e, \frac{T_w}{T_0}) = \frac{B}{2} e^{x'+y'}\left(1 - Erf\left(\sqrt{x'} + \frac{y'}{2\sqrt{x'}}\right)\right) + \frac{C}{2} e^{4x'+2y'}\left(1 - Erf\left(2\sqrt{x'} + \frac{y'}{2\sqrt{x'}}\right)\right) \tag{72}$$

These equations exhibit the proper limiting behavior; for example, in the limit $x' = 0$, eq. (71) reduces to (67) and (68), while in the limit $x' = \infty$, it reduces to (48). It is equally easy to show that equations (71) and (72) are asymmetric relative to y', and that at $y' = 0$ the $\bar{u}$ obtained from (71), that is

$$\bar{u}(x', y'=0; P=0) = \frac{1}{2} e^{x'}\left(1 - Erf\sqrt{x'}\right) \tag{73}$$

does not represent the apex of the profile as it did in the symmetric case (in References 5 and 6, eq. (73) was called the "pseudodefect"). In the present case, the velocity defect is defined as

$$w \equiv 1 - \frac{u_c}{u_e} = w(x', 0; P=0) \tag{74}$$

where u_c is the minimum velocity at any x', herein also called the "center" velocity. Then the velocity profile is

$$\tilde{u} \equiv \frac{u_e - u}{u_e - u_c} \tag{75}$$

The center velocity u_c as well as the position y'_{cu} (the "center position") at which it occurs cannot, unfortunately, be derived in closed form. It will therefore be discussed in connection with the computations of Section 7.

The discussion of the asymmetric temperature field follows quite closely the above discussion for the velocity. The definition of the temperature defect, decrement, profile, etc. follows the rule that the symbol (0) used for the symmetric wake (eqs. (45), (56), etc.) is now changed to a subscript c. Note, however, that the apex of the temperature profile is again impossible to derive analytically in closed form. We therefore have no "a priori" evidence that the wake center found from the temperature profile coincides with the wake center y'_{cu} discussed earlier for the velocity profile. This point will be clarified in the computations presented in Section 7.

The remaining properties of the completely asymmetric wake such as the density can also be presented in the form of defects, profiles, etc. defined as for the symmetric wake but with subscript "c" in place of the symbol (0). Results will be shown below.

6. Computations and Graphic Results for the Symmetric Wake

The formulas derived in Section 5 for the symmetric wake (P = 1) have been utilized to present graphically the behavior of the fluid properties in such a wake from the T.E. ($x' = 0$) to far distances downstream. These, which are shown on Figures 4 through 16 and which will be discussed briefly in this Section, were obtained by numerical computations with the programs shown in the Appendices.

The chief interest here lies in the way the flow adjusts from a discontinuous profile at the T.E. to a continuous, analytic profile immediately past the T.E. We are also interested in the speed with

which the asymptotic solutions (48), (49), etc. are attained. We are no less interested in the effect of stream Mach number M_e and of the temperature ratio T_w/T_o on these adjustments. In this respect, it should be recalled that the fluid velocity is, in the compressible transformation of eq. (16), unaffected by M_e or T_w/T_o, but that the thermodynamic variables are strongly affected by these parameters.

It is well to keep a physical perspective of the distances involved downstream of the T.E., and in this sense the kinematic boundary layer thickness δ is a more meaningful length measure. For example, suppose we are interested in the flow in a gas-dynamic laser cavity 10 cm. downstream of the nozzle array. Suppose, further, that the nozzle exit Mach number is high-supersonic with a laminar δ = 0.5 mm. In this case, the ratio δ/θ is of order 20, while Re_θ can be taken to be 400 (i.e. near the upper limit for laminar flow). Then, from eq. (36):

$$x' \equiv \frac{x^*}{\Theta Re_\Theta} = \frac{x^*}{4\theta\, Re_\theta} = \frac{x^*}{4\frac{\theta}{\delta}\delta\, Re_\theta} = \frac{10}{4\frac{0.5}{20}\,400} = 0.25 \qquad (76)$$

In this example we see, therefore, that the range $x' < 1$ is of major practical interest.

Figures 4 and 5 show the velocity defect according to eq. (47). The experimental points on Figure 5 will be discussed later, but the comparison with other theories is in order at this point. Specifically, the good agreement with Goldstein's theory (Ref. 2) should be noted, as well as the difference from the "asymptotic solution", i.e. eq. (48). The latter seems to be adequate in giving $\tilde{w}(x')$ beyond $x' = 1$, but expectedly fails to do so at $x' < 1$. Figure 4 demonstrates, by the proximity of the solid to the dashed curves that for very short distances past the T.E. the profiles are still almost identical with the initial profiles $\tilde{u}_o$, $\tilde{T}_o$ marked "theory". (the solid curve for $\tilde{u}$ has a rounded apex not visible on this graph). The evolution of the velocity profile $\tilde{u}$ is shown on Figure 6. The use of two different abscissas in this Figure is necessary to show how the profile approaches the similarity solution (49), occurring past $x' = 1$ as noted.

There are infinite combinations possible of M_e and T_w/T_o which can be used to examine the behavior of the defects, decrements, and profiles of the thermodynamic variables according to eqs. (51), (55), (56), etc. of Section 4. Generally, computer runs with the programs shown in the Apprendices were restricted to M_e = 0, 2, 4, and 6, and T_w/T_o values of 0.2, 0.6, 1, 1.4, and 1.8 (the "cooled", "adiabatic" and "heated" wake).

The temperature-decrement plots of Figures 7 and 8 indicate the significant finding that the wake behavior subdivides naturally into two categories. The first is the high-M_e, highly cooled type of wake (Figure 7) which is also the one of practical importance in laser applications. Here the decrement is "normal for $M_e < 4$, but between $M_e = 4$ and 5, the decrement switches sign---in some measure due to the definition of the decrement. For all other cases, however, the behavior is typically shown on Figure 8 ; the decrement decreases monotonically from the T.E., and is always included within the band defined by each pair (solid and dashed) of curves. For example, for adiabatic or heated wakes ($T_w/T_o > 1$) and at $x' = 1$, the decrement always lies between 0.25 and 0.35 regardless of M_e.

The effect of compressibility and heat transfer on the temperature profile is shown by the three plots of Figures 9, 10, and 11. The effect of high M_e alone or T.E. cooling alone does not create any unusual behavior in $\bar{T}$ as Figures 9 and 10 indicate; the adiabatic hypersonic wake is simply thicker than its low-speed cooled counterpart. When high M_e is combined with cooling, however, Figure 11 shows that the profile has large off-axis peaks in the temperature, inherited from the non-monotonic initial temperature distribution at the T.E. (see dashed curves in Figure 3 and also in the upper portion of Figure 11).

The density and total temperature defects are shown on Figures 12 and 13. Note that for $M_e = 5$ and $T_w/T_o = 0.2$, the density defect increases quickly from 0.16 to 0.52 a short distance ($x' = 0.05$) downstream of the T.E. and thereafter decreases monotonically.

Figures 14 and 15 illustrate the differences among velocity, temperature, and density in the speed with which each tends to achieve the asymptotic state. The high-supersonic, cooled-wake environment has been selected for these examples. Figure 14 plots the three defects together with their asymptotes (i.e. eqs. (48) and (53)), since the latter are sometimes used as approximations to the actual defects. We see that by $x' = 0$ the actual velocity defects are within 15 percent of their asymptotic approximations, but that the density defect is closer to one-half of what its asymptotic formula predicts. Similarly, for $x' = 0.1$ Figure 15 shows that the density wake is considerably thicker than the velocity wake, with the temperature wake falling between the two. Note that these differences would be even more prominent if the Prandtl number had not been taken as unity.

Finally, Figure 16 shows the physical "velocity half-thickness" b* for two different Mach numbers and temperature ratios. The b* is defined as the distance from the wake plane of symmetry and the point whre $\bar{u}$ is 0.01, and was computed using a transformation inverse to that of eq. (16). We see that (a) the wall temperature does not much affect the low-speed wake thickness, but it does so for $M_e = 6$, (b) the high-speed wake is thicker by a factor of 2 to 4 than the low-speed one depending on T_w/T_o (this is really the effect of the initial δ/θ) and (c) the wake grows by only a small amount (about a factor of 2 at most) before x' becomes unity.

The above results illustrate the findings of Section 5 that the present theory achieves two major goals: an uneventful transition from the discontinuous T.E. profile, and agreement with the classical asymptotic behavior at large x'. Regarding the latter, the early papers (Ref. 7) indicate that the asymptotic solution is reached within about "three plate lengths" (i.e. $x^* = 3\ell$) of the hypothetical flat plate of length ℓ generating the wake. We can check to see if the present theory agrees by connecting our coordinate x' with the equivalent normalized distance x^*/ℓ. Using the customary incompressible formula for the T.E. θ in terms of ℓ:

$$\theta^2 Re' = (0.664)^2 \ell$$

we get, from eq. (36):

$$X' \equiv \frac{x^*}{\Theta Re_\theta} = \frac{x^*}{4\theta Re_\theta} = \frac{x^*}{4\theta^2 Re_\theta} = \frac{x^*}{4(.664)^2 \ell} = 0.56\,\frac{x^*}{\ell}$$

At $x^*/\ell = 3$ or $x' = 1.68$ our present theory (eq. (47) or Figure 4) gives $w = 0.206$, while the asymptotic value from eq. (48) is 0.218 for a difference of only about 5 percent; thus the three-plate-length estimate still holds. On the other hand, the corresponding comparison for the density defect is 0.345 and 0.589 for the actual and asymptotic values respectively, for a difference of 70 percent (assuming $M_e = 5$ and $T_w/T_o = 0.2$).

7. Computations and Graphic Results for the Asymmetric Wake

As already noted, the computations for asymmetry were limited to the extreme case of $P = 0$. To keep this report to a reasonable size, numerical computations with eqs. (71), (72), etc. were done for three cases: $M_e = 6$, $T_w = 0.2T_o$; $M_e = 0$, $T_w = 0.2T_o$; and $M_e = 6$, $T_w = T_o$. Comparison of the former two allows an appreciation of the compressibility effect, while the heat-transfer effect can be illustrated to some extent by comparing the first with the third cases. Of course, the results for the velocity are valid for all M_e and T_w/T_o because of the transformed coordinates.

A general illustration of the course of events beyond the trailing edge is given by Figures 14 through 21 which include the initial variations (at the T.E.) of the variable plotted. Note that these initial variations are uniformly zero for all $y' > 0$, since $P = 0$ implies that $\theta_1 = 0$ if θ_2 is finite; that is, there is no boundary layer, initially, on the positive half-plane. Also note that in these Figures, the plotted quantities are the variations $1 - u/u_e$ etc. rather than the profiles as defined by eq. (75) etc.

Just as in the symmetric wake, the discontinuity vanishes as soon as the fluid leaves the T.E., the "rounded top" of each variation marking the "wake center". The T.E. asymmetry persists for some distance, symmetrization occurring gradually toward the larger x'. The wake center deflects into the $y' < 0$ half plane; for the velocity, which always starts out with the center at $y' = 0$ the deflection is gradual. For the temperature, the $M_e = 6$, $T_w = 0.2T_o$ case shown in Figure 20, the center initially lies off the

$y' = 0$ plane, i.e. at infinite x' the wake symmetrizes but remains displaced off the $y' = 0$ plane. For cases of practical interest, as Figure 20 shows, the deflection does not amount to more than one or two . However, the fact that the wake center for the velocity, called y'_{cu}, does not coincide with that for the temperature or density (y'_c , y'_c respectively) is a major finding of this work. Figure 22, on which the deflections of y'_c , y'_c , and y'_c are drawn, shows that the centers for these three properties remain deflected along different paths as x' becomes infinite. This difference in the wake center of velocity, temperature, and density lies in the fact that whereas the velocity center is always at $y' = 0$ when $x' = 0$, the extremum in the temperature distribution at the T.E. may be off the $y' = 0$ plane (the case of the cooled hypersonic wake discussed here is a typical example).

The above remarks refer to the compressible-transformed deflection; in the physical plane, the wake centers (for the velocity only) are shown on Figures 23, 24, and 25. It was found that in the physical plane, the deflection decreases at large x' generally, i.e. the wake centers tend to return to $y' = 0$. Since the deflection amounts to only a small physical distance anyway, it probably deserves little additional discussion. Finally, in the non-dimensional coordinate F defined by eq. (50), the wake centers for all variables seem to always return to $y' = 0$.

Figures 26, 27, and 28 show the net result of the asymmetry on the maxima or minima of the flow variables at the wake center. This is expressed in terms of the defects such as of eq. (44), (51), etc. except that the center property, being off-axis, is designated by the subscript "c". Dashed lines on these Figures represent the symmetric-wake defects from eq. (44), (51), etc. for comparison. It is seen that even the largest asymmetry does not produce changes in the defects of any more than a few percent, and these changes naturally vanish at large x'.

Figure 29 shows examples of the developing profile, while Figure 30 shows how fast the asymmetric profiles approach the asymptotic limit expressed by eq. (49). The example chosen is $M_e = 6$, $T_w = 0.2T_o$ and

$x = 1$, that is near the region where the symmetric wake itself ($P = 1$) was beginning to coincide with the asymptotic profile. The ordinate is normalized with the center deficit $u_e - u_c$ or $T_c - T_e$, while the abscissa $F - F_c$ where

$$F_c \equiv \frac{y'_c}{2\sqrt{x'}},$$

is shifted to put the top of the profile at zero. It is seen that at $x' = 1$, only slight evidence of the asymmetry still remains, and that all profiles regardless of P value are nearly the same as the asymptotic one.

Finally, Figures 23, 24, and 25 show the geographical features of the $M_e = 6$, $T_w = 0.2T_o$ wake in the physical plane, consisting of the wake edges b^*/Θ in the two half planes and the physical wake center y_c^*. The edges and the center were again computed by the transformation inverse to (16), and are limited to the velocity field; that is the edge is the position where the velocity profile is 0.01, while the center is the maximum of the velocity profile (one could equally well draw analogous curves for the temperature and the density). The following are obvious from these Figures: (a) the initially zero-thickness portion of the wake grows rapidly, while the initially finite half (the one with initial momentum thickness θ_2) grows slowly and on occasion decreases slightly in thickness at the beginning, (b) the wake center originally deflects downwards and then returns toward the plane $y' = 0$, (c) the asymmetry decreases downstream since the two edges begin becoming equidistant and (d) the wake thickness in terms of Θ is independent of P at large x'.

8. Discussion and Comparison With Experiments

The present work was motivated largely by the desire to provide closed-form solutions for the symmetric wake for application to gas-dynamic lasers. In an earlier paper (Reference 8) the present author formulated a theoretical compendium of wake predictions for compressible two-dimensional wakes at arbritrary M_e and T_w/T_o. This earlier theory was based on an integral approximation to the total drag of and heat loss from the structure

separating the two streams, as well as the asymptotic symmetric wake formulas contained herein (eq. (48), (49), etc.) Experiments by Peterson (Reference 9) and this author (Reference 10) produced data agreeing with the turbulent-wake prediction of this earlier theory but disagreeing with its laminar counterpart. This could be explained by the fact the turbulent wake mixes so quickly that its non-equilibrium (adjustment) zone behind the T.E. never plays a role; for the laminar wake, however, the non-equilibrium zone (found herein to extend as far as $x' = 1$ to $x' = 3$) was unaccounted in the early theory, thus producing disagreement with the data. It therefore became important to have on hand a wake theory treating equally the asymptotic, far region as well as the non-equilibrium ("near" or "adjustment") region close to the T.E.

The same data of Reference 10 disagreeing with the earlier theory of Reference 8 are plotted on Figure 5 . Two data points from Sato and Kuriki (Reference 11) are also included. The agreement is very good within the data scatter. No other quantitative data could be found for comparison, but neither could intimations be found in the literature contradicting the present findings. In fact, Batt and Kubota (Reference 12) present an experiment frequently intimating the validity of the present approach; for example, they find that the proper scaling length is the total T.E. momentum thickness.

Both Figures 4 and 5 show how, in the limit $M_e = 0$, $T_w = T_o$, the present theory agrees with the findings of Tollmien and Goldstein for the entire x' range. This agreement, as well as the agreement with the data, refers to the symmetric wake. No previous theoretical or experimental threatment of the asymmetric wake could be found.

Note should be made of the differences between the adjustment of the density field, and the adjustment of the other flow variables. The density is generally very slow to adjust to the asymptotic limit. The reader can expand on this statement by making numerical computations with the programs listed in the Appendix.

The good analytic behavior of the solutions presented here, and the agreement with the data appear, at first glance, to be disproportionate to the severity of the basic assumptions (10) and (11). Recall, however, that the solutions are forced to obey the correct boundary (initial) conditions at the T.E., while the method supplied by Gold guarantees the proper asymptotic behavior as well. With the solutions thus "tied down to the proper limits at the two ends", it is not surprising that the intermediate regions give the proper results.

9. Conclusions

1. Closed-form, analytic solutions have been found for steady, laminar two-dimensional wakes applicable for any value of the edge Mach number M_e, trailing-edge, wall-to-stagnation temperature ratio T_w/T_o and for any ratio P of the momentum thickness of the two merging boundary layers. The streamwise development of the wake is controlled by the total momentum thickness and the unit Reynolds number contained in the longitudinal variable x'.
2. Beyond a certain distance x' ranging from 1 to 3 the wake conforms to the classic similarity form regardless of M_e, T_w/T_o or the initial asymmetry expressed by P. This distance marking the onset of dynamic "equilibrium" is almost exactly equal to that found in early studies with incompressible flows. Only the density lags behind the other flow variables in reaching equilibrium within this distance.
3. Many, if not most, current practical applications involve wakes within the "non-equilibrium" distance between the trailing edge and $x' = 1$ to 3. The classic asymptotic formulas are inapplicable in this region. For wakes such as encountered in laser cavities (large M_e, $T_w << T_o$) the present theory reveals many peculiarities of behavior, such as non-monotonic development, off-axis maxima etc. even for the initially symmetric wake.

4. Even for the largest initial asymmetry, the flow defects (e.g. minimum velocity) are almost equal to those of the symmetric wake. In the non-equilibrium region, however, the initial asymmetry causes the wake to deflect towards the side of the initially thicker boundary layer, and the extrema in the velocity profile do not coincide with the extrema for the density or temperature.

REFERENCES

1. Tollmein W.: "Grenzschichten", Hankdbuk der Exper. Physik IV, Part I, P. 267 (1931).

2. Goldstein S.: "On The Two-Dimensional Steady Flow of a Viscious Fluid Behind a Solid Body - I", Proc. of the Royal Society of London, Series A, Vol. 142, p. 545 (1933); also: "On The Two-Dimensional Steady Flow of a Viscious Fluid Behind a Solid Body - II", Proc. of the Royal Society of London, Series A, Vol. 142, p. 563 (1933).

3. Kubota T.: "Laminar Wakes With Streamwise Pressure Gradient", GALCIT Hypersonic Research Project Memo No. 9, CIT, Pasadena, CA, May (1962).

4. Gold H.: "Laminar Wake With Arbritrary Initial Profiles", AIAA J., Vol. 2, No. 5, p. 948, May (1964).

5. Demetriades A.: "Development of the Arbritrary Two-Dimensional Non-Equilibrium Laminar Wake", Montana State University, MSU/SWT IM 80 - 4, December (1980).

6. Demetriades A.: "Development of the Arbritrary Two-Dimensional Non-Equilibrium Laminar Wake", TETRA Corp. Report TR 81-005, Albuquerque NM, June (1981).

7. Schlichting H.: "Boundary-Layer Theory", McGraw-Hill Book Co., New York (1955), pp. 138-142.

8. Demetriades A.: "Linearized Analysis of Gasdynamic-Laser Wakes With Applications", J. of Energy, Vol 1, No. 2, pp. 73-74, March-April (1977).

9. Peterson C.W.: "Measurements of Flowfield Properties in a Gasdynamic Laser Nozzle Wake", AIAA J., Vo. 17, No. 8, p 854, August (1979).

10. Demetriades A.: "Experimental Test of the Theory of GDL Nozzle-Cusp Wakes", Aeronutronic Report U-6395, Newport Beach, CA, (1978).

11. Sato H. and Kuriki K.: "The Mechanism of Transition in the Wake of a Thin Flat Plate Places Parallel to a Uniform Flow", JFM Vol. II, Part 3, pp. 321-352, November (1961).

12. Batt R.G. and Kubota T.: "Experimental Investigation of Laminar Near Wakes Behind 20^{o} Wedges at M = 6", AIAA J., Vol. 6, No. II, November (1968).

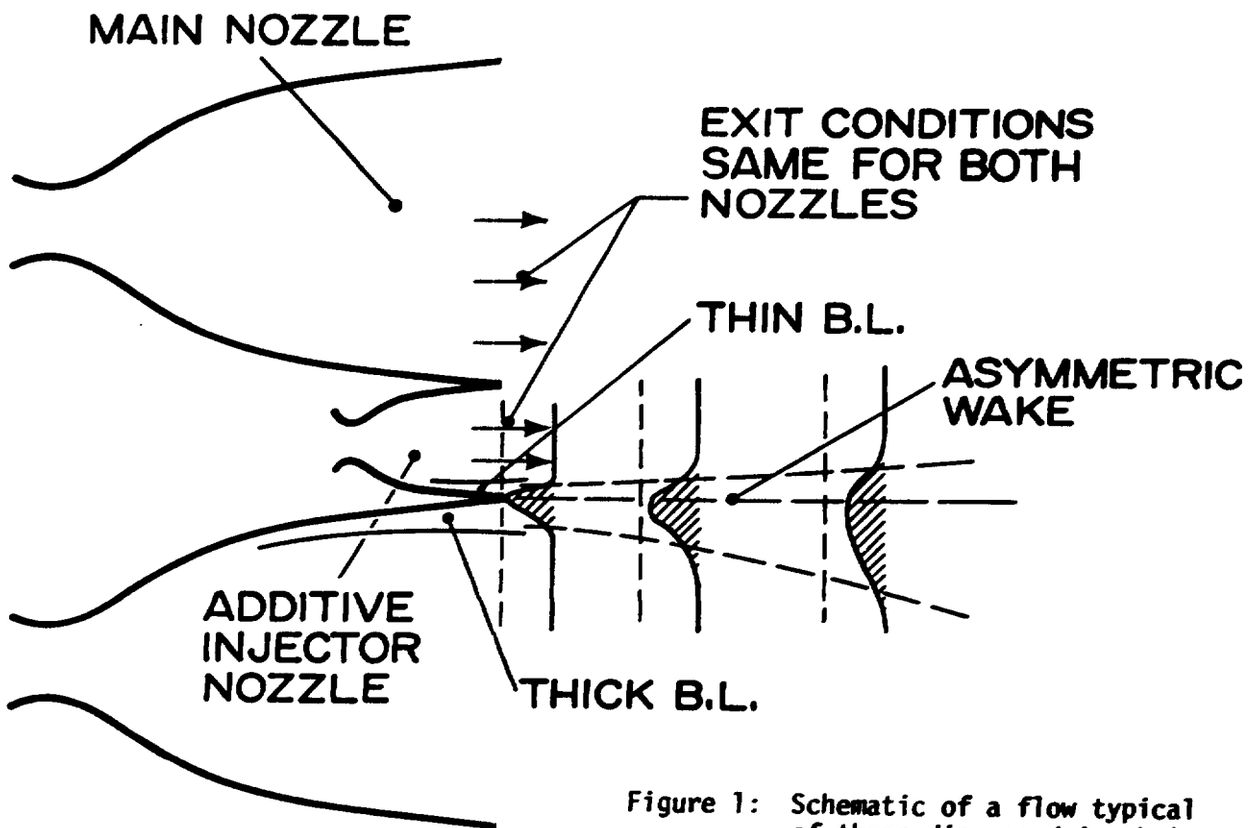

Figure 1: Schematic of a flow typical of those discussed in the present report.

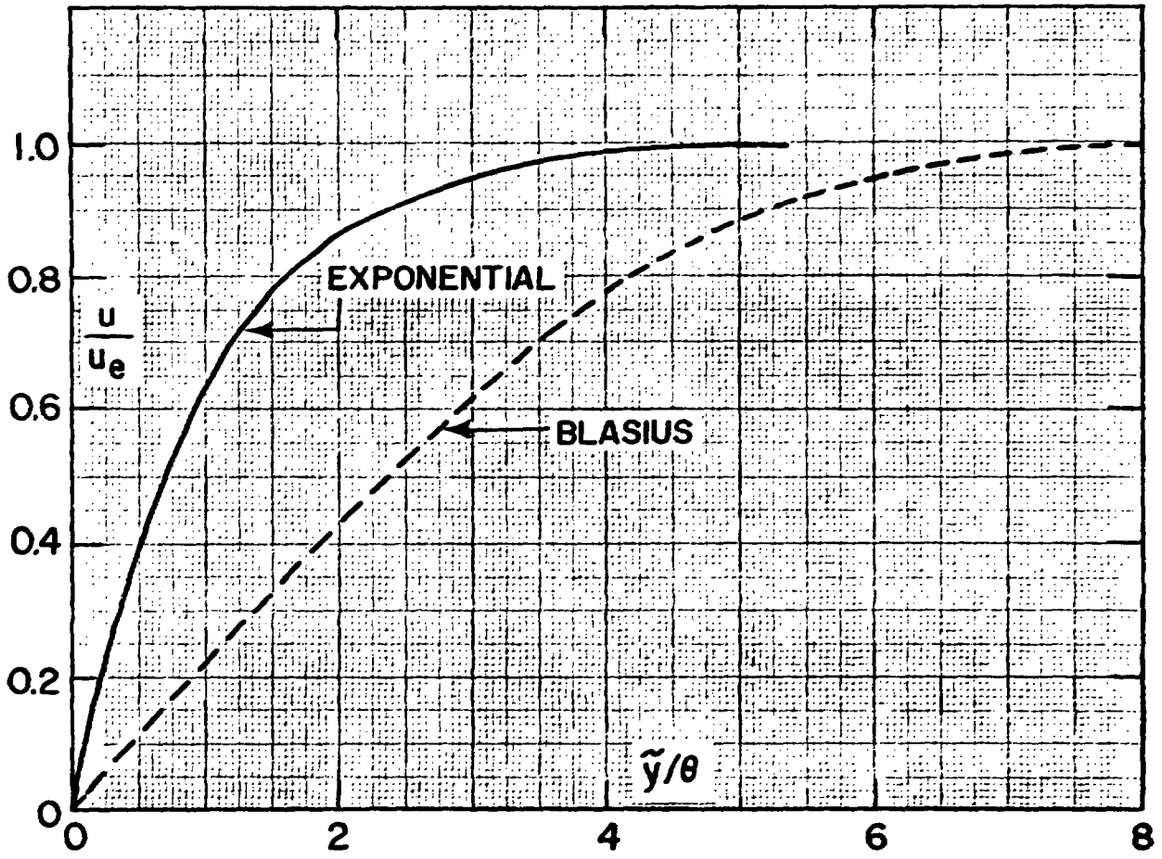

Figure 2: Initial velocity profile (exponential).

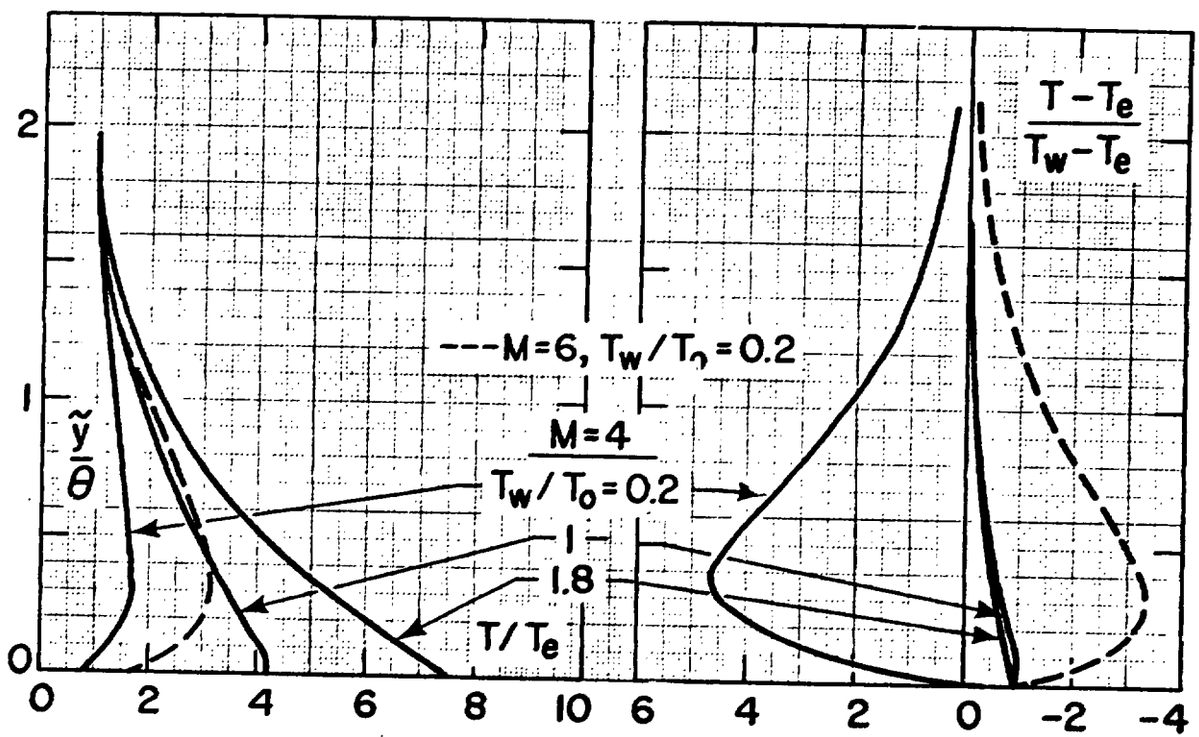

Figure 3: Temperature profiles of the type resulting from the assumed velocity profile and the Crocco relation.

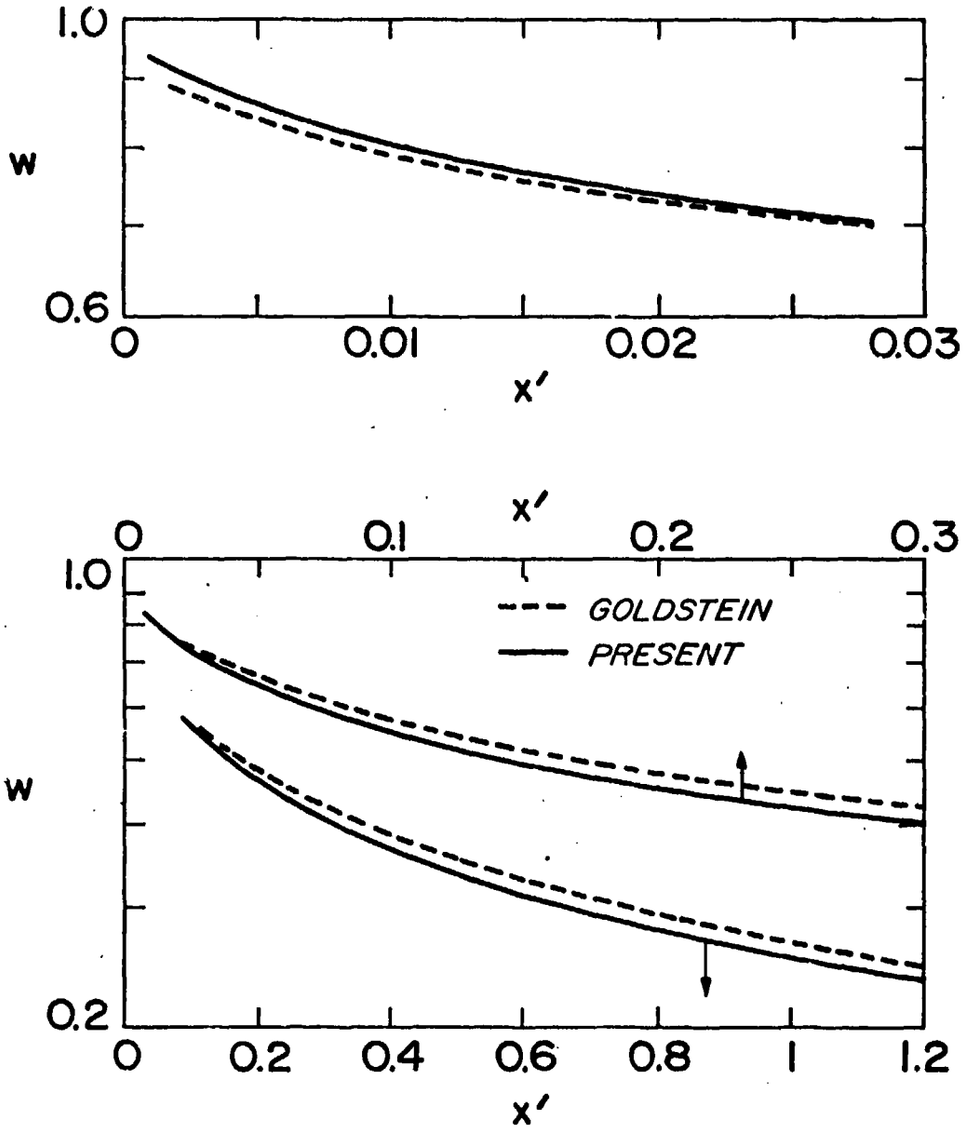

Figure 4: Symmetric wake velocity defect compared with that due to Goldstein.

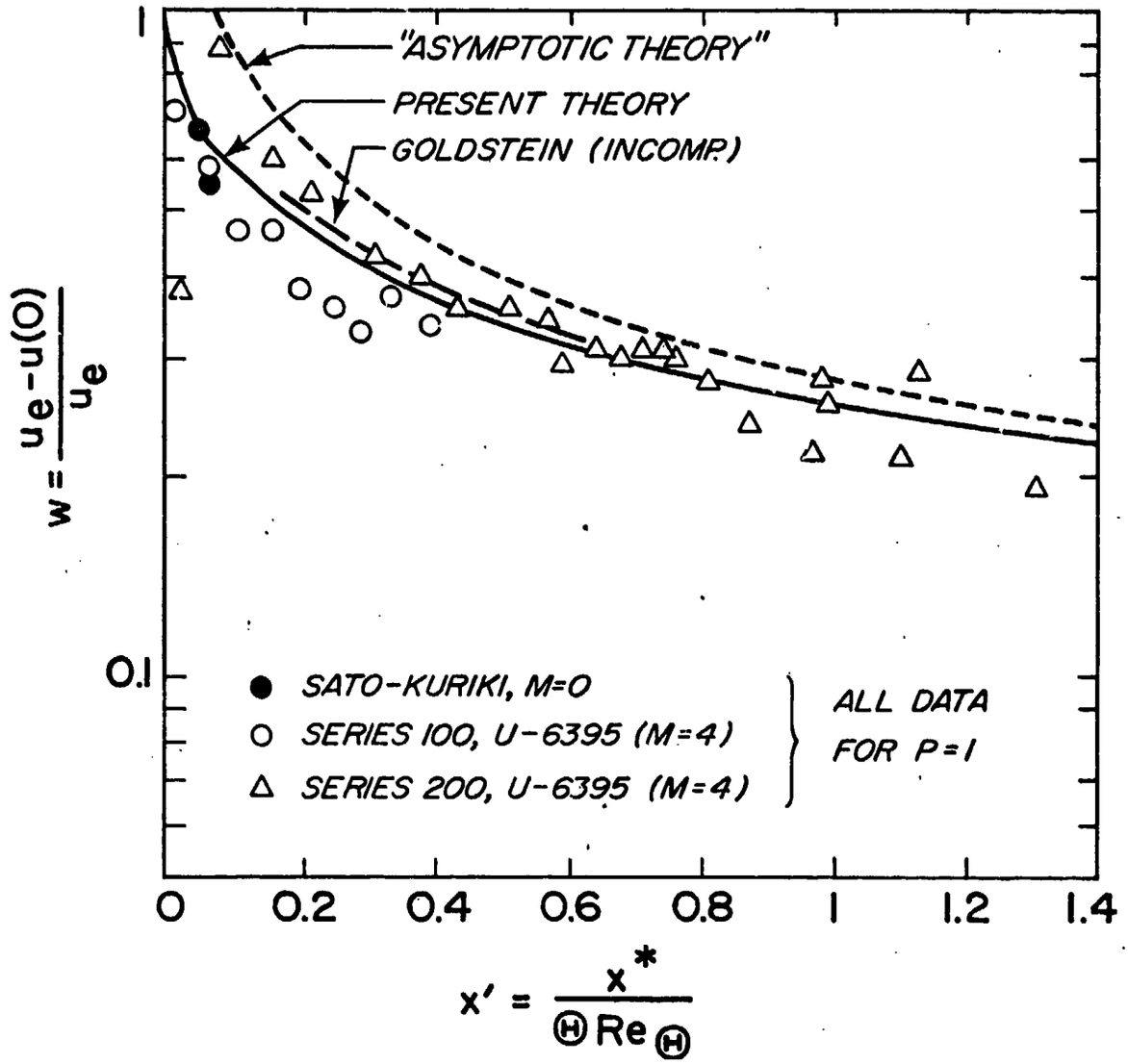

Figure 5: Theoretical and experimental review of velocity defects for symmetric wakes.

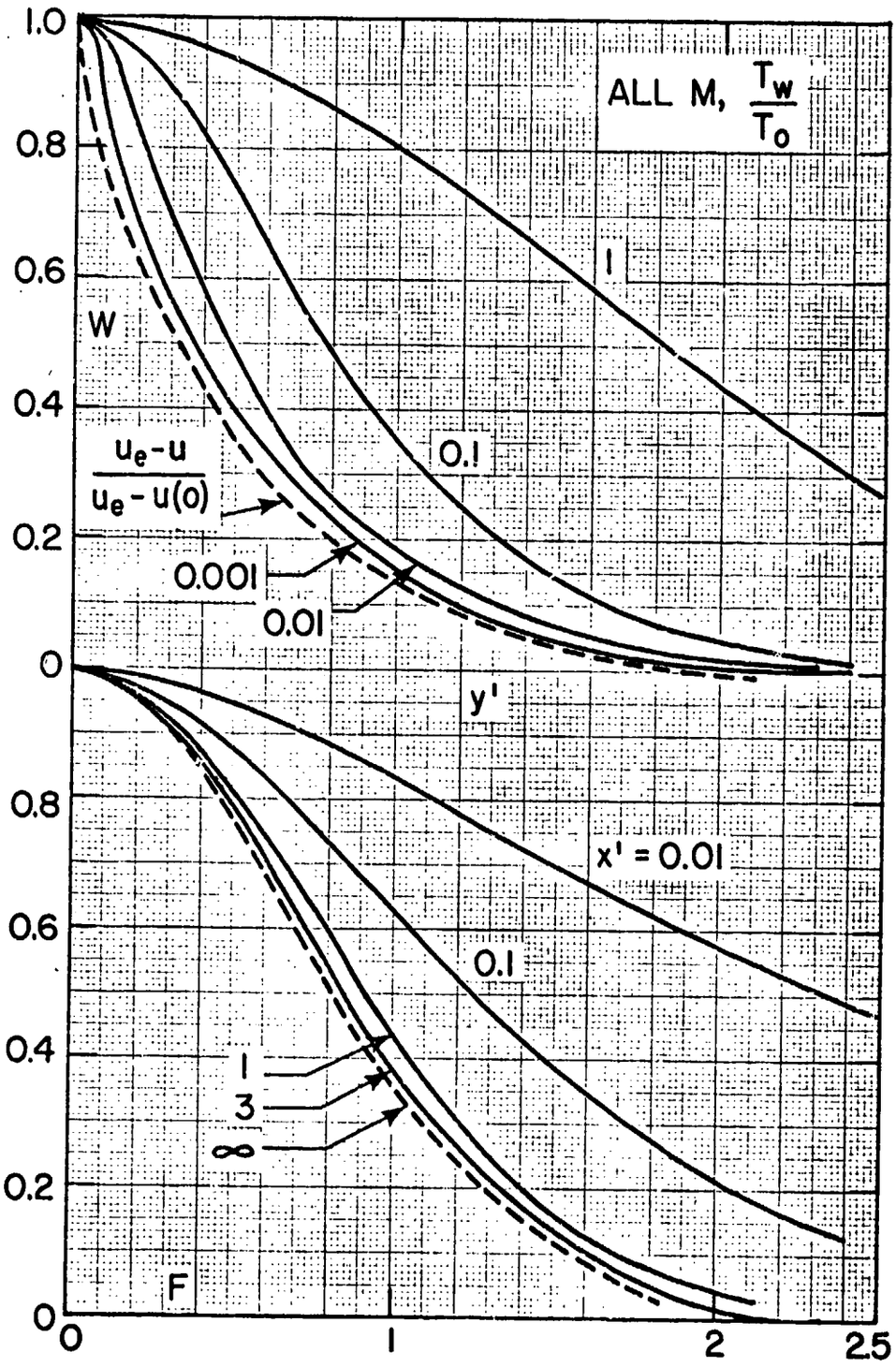

Figure 6: Symmetric wake velocity profiles.

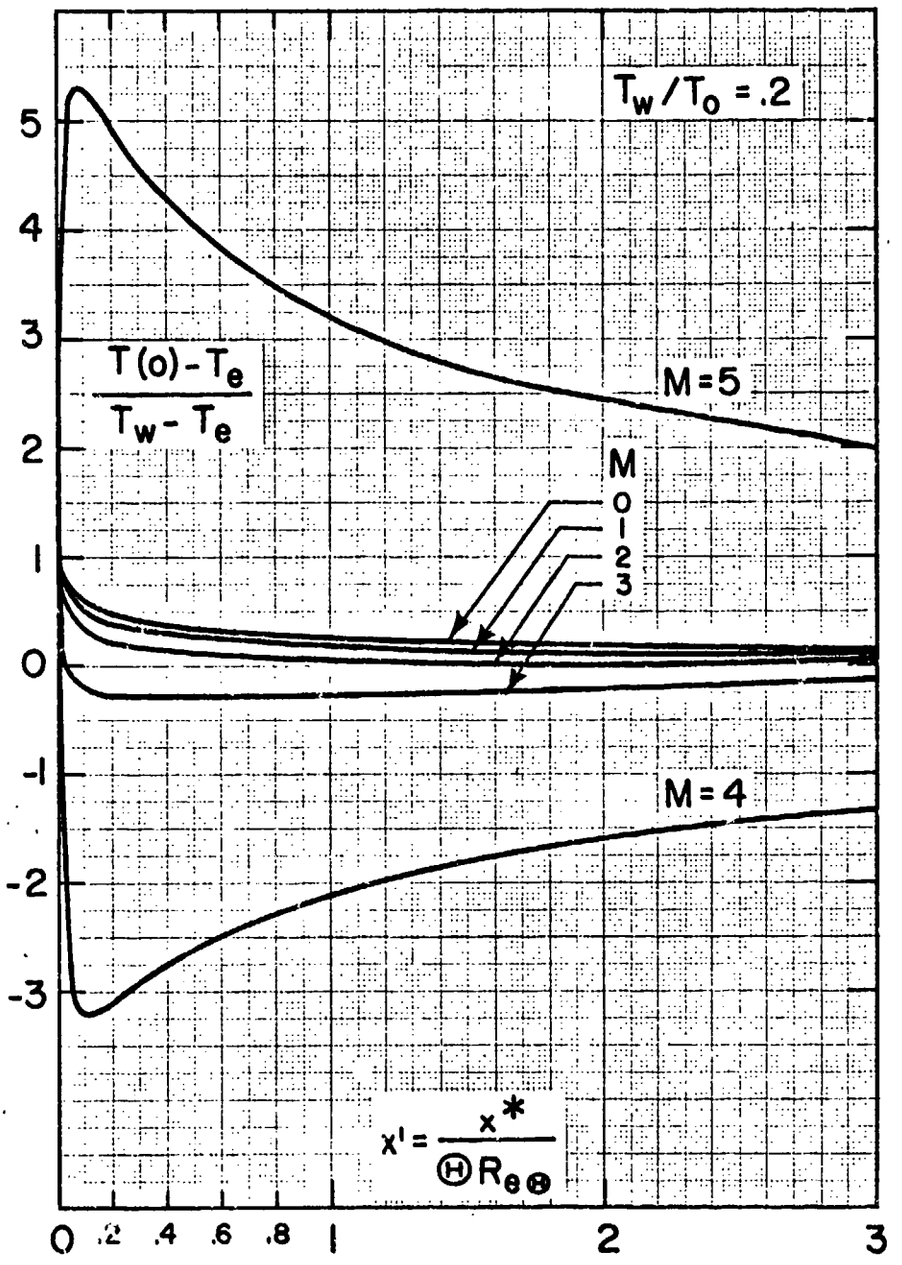

Figure 7: Temperature decrement for cooled symmetric wakes.

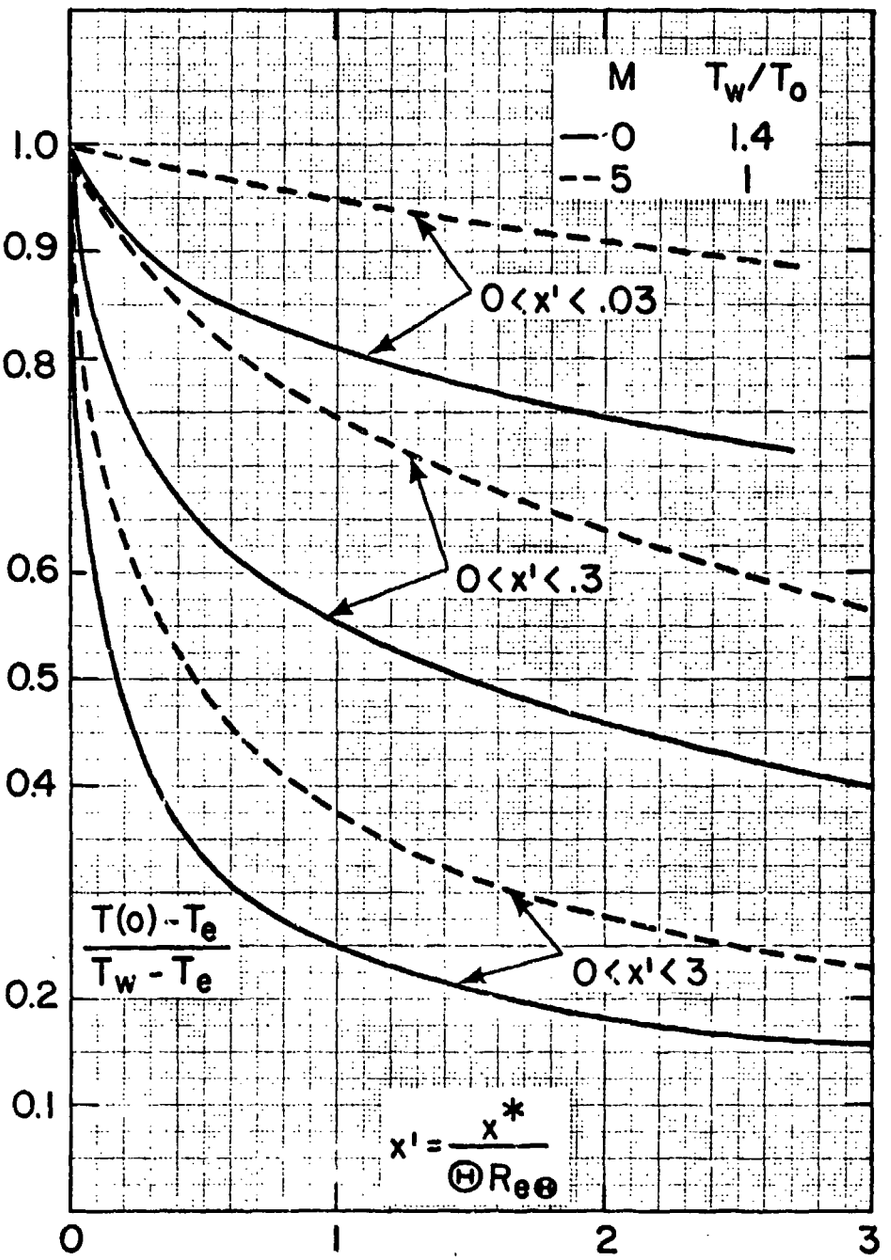

Figure 8: Temperature decrement of adiabatic and heated symmetric wakes. Solid and dashed curves represent extreme variations.

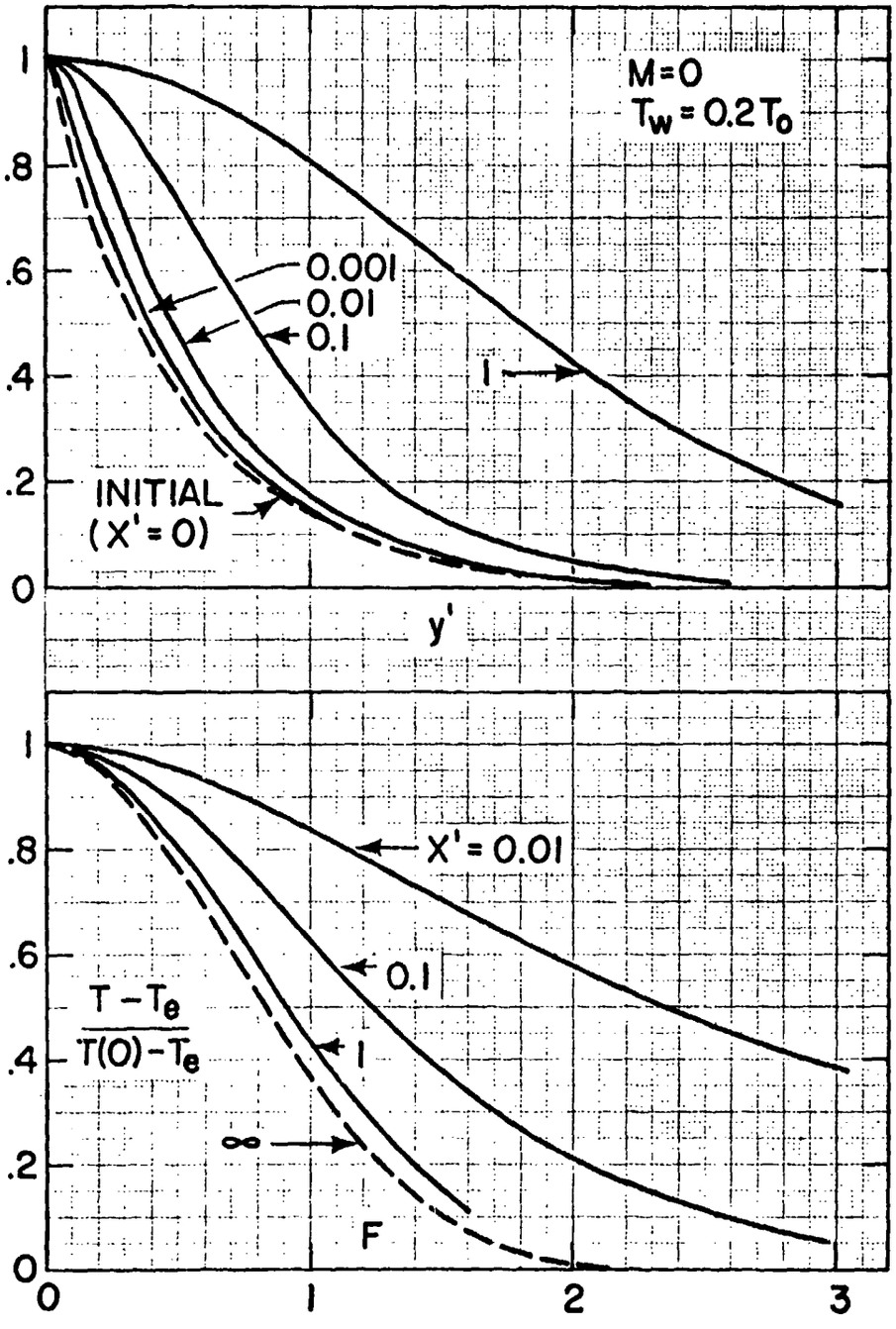

Figure 9: Temperature profiles for the low-speed, cooled symmetric wake.

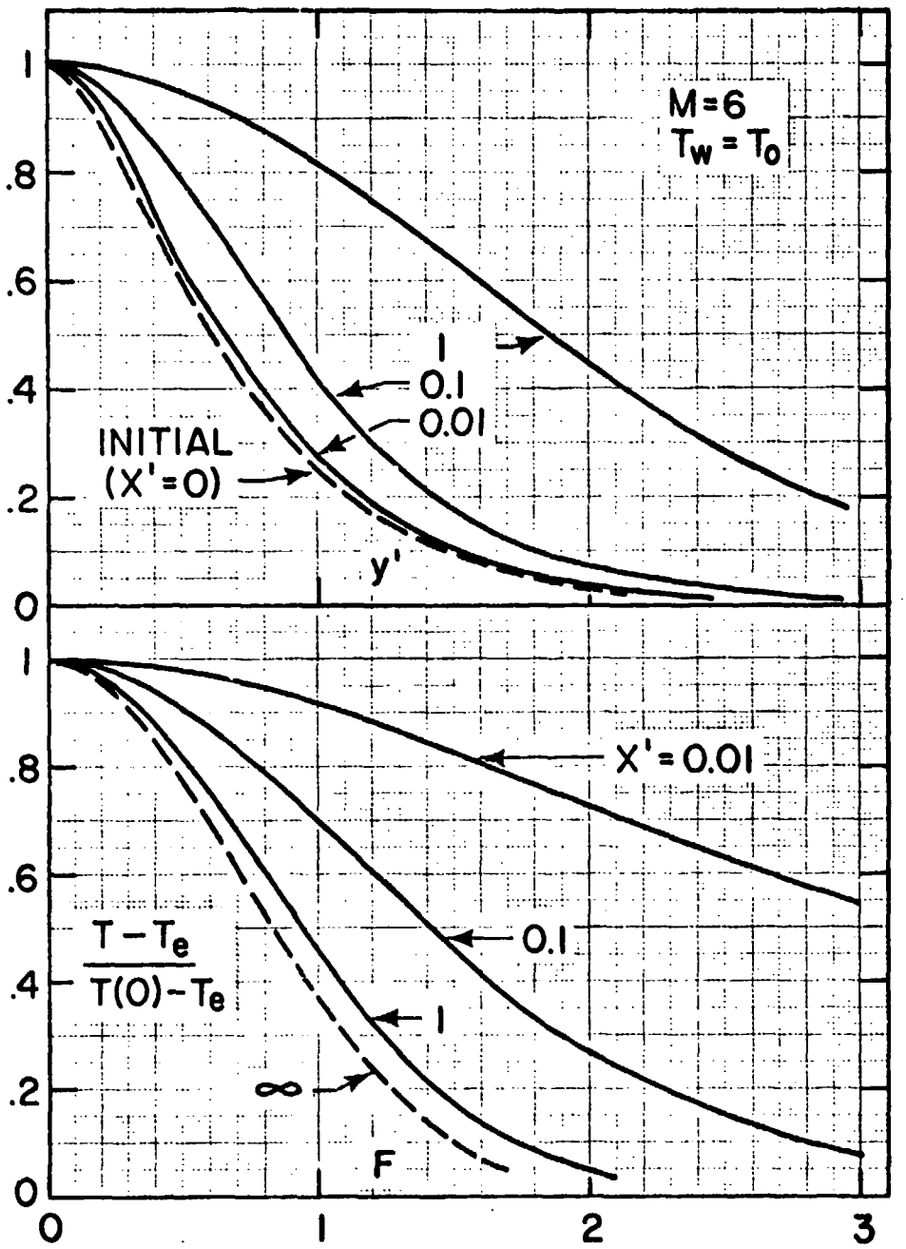

Figure 10: Temperature profiles for the hypersonic, adiabatic symmetric wake.

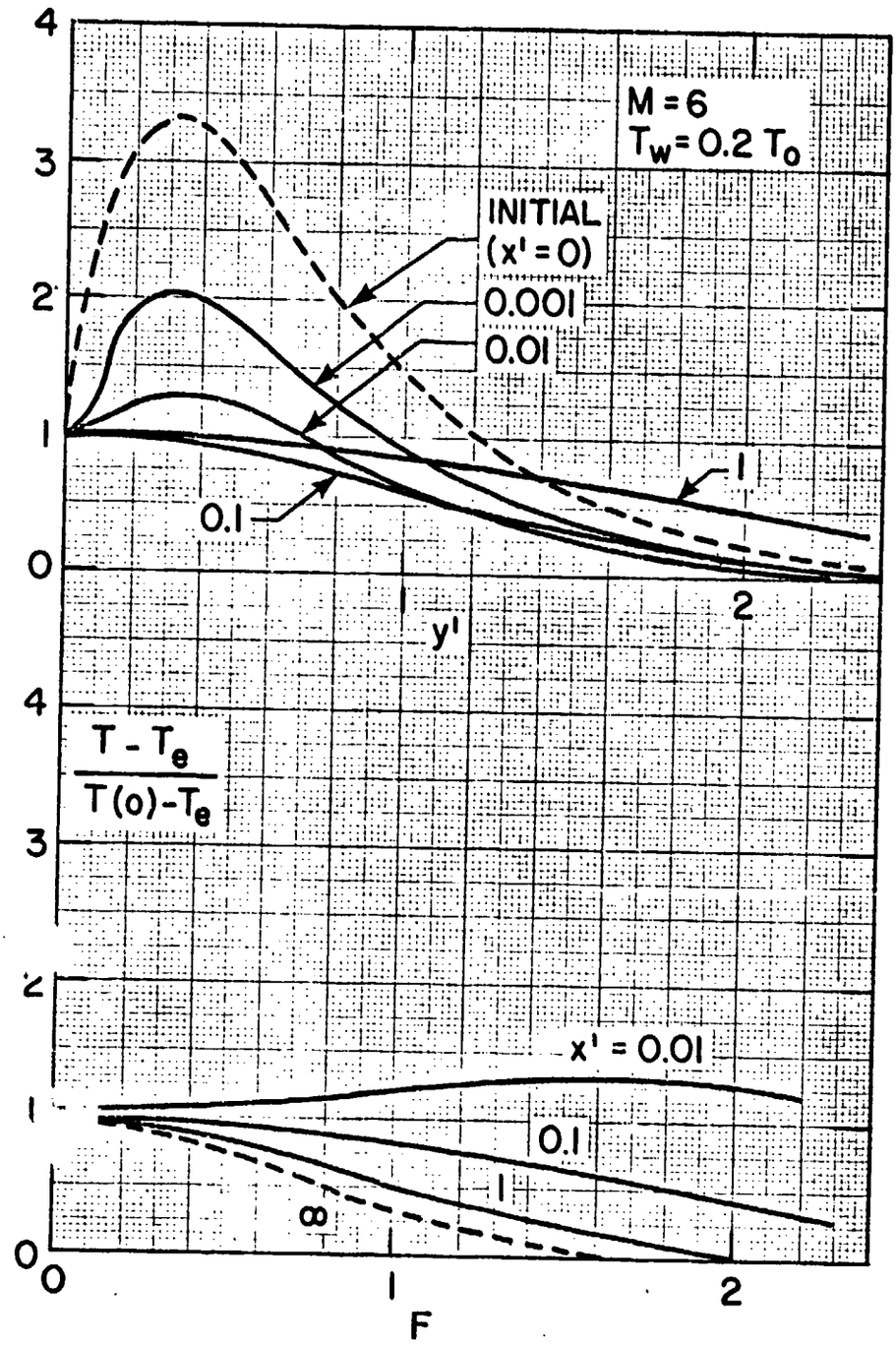

Figure 11: Temperature profiles for the hypersonic, cooled symmetric wake.

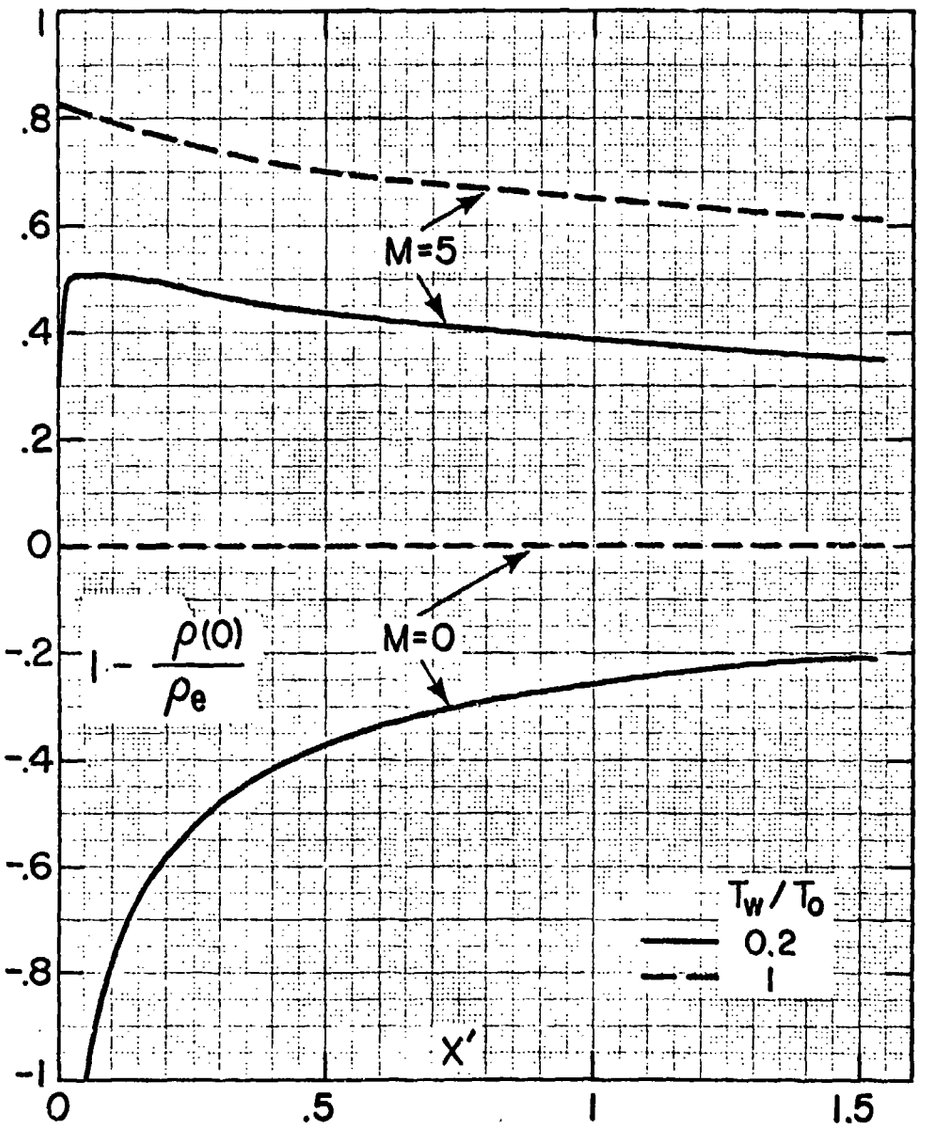

Figure 12: Density defects for the symmetric wake (typical).

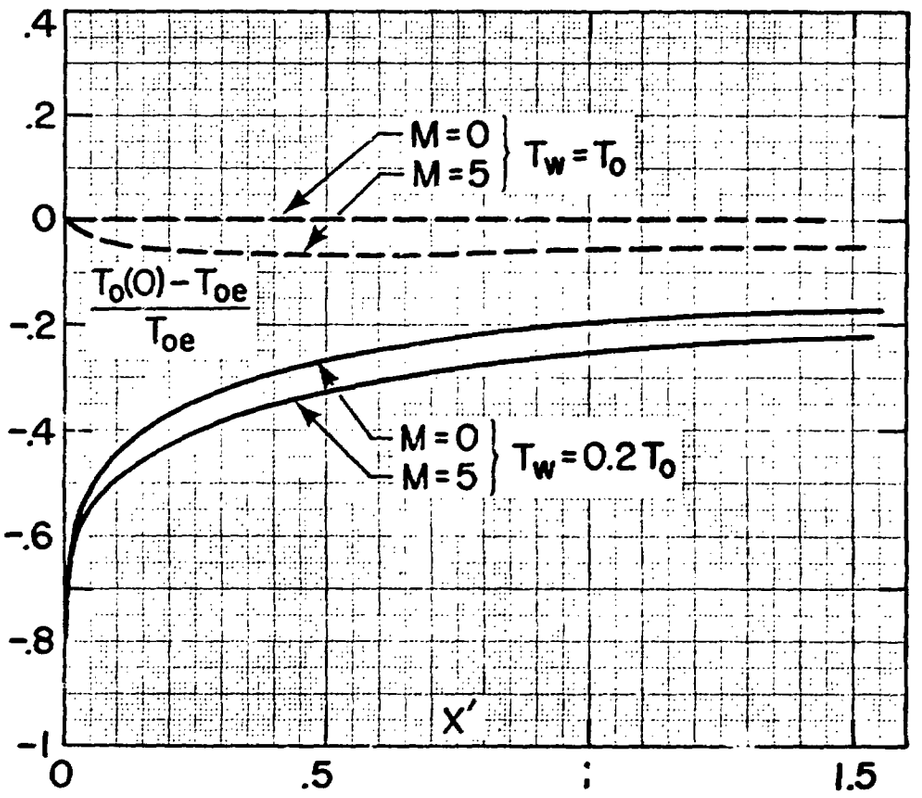

Figure 13: Typical total temperature defects for the symmetric wake.

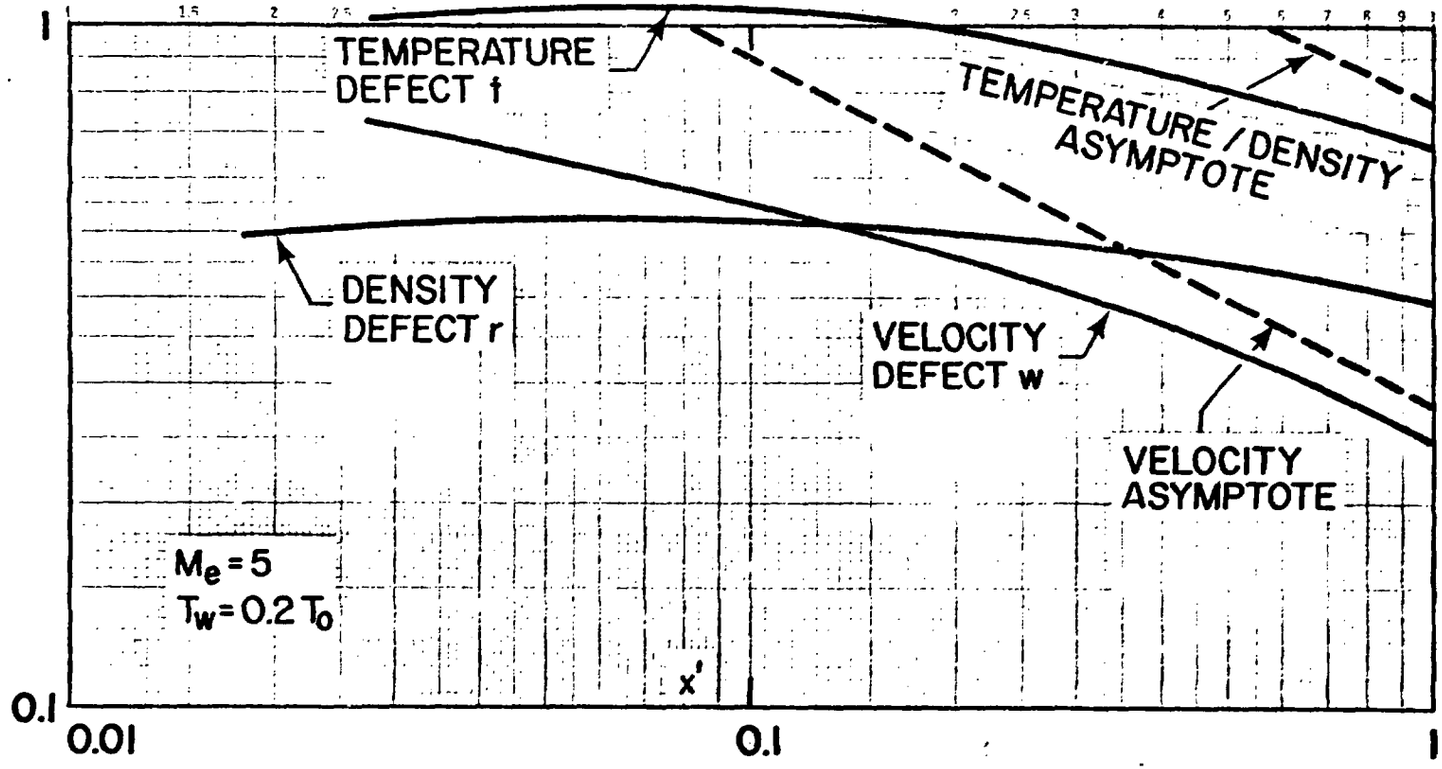

Figure 14: Relative behavior of the defects for the supersonic cooled symmetric wake.

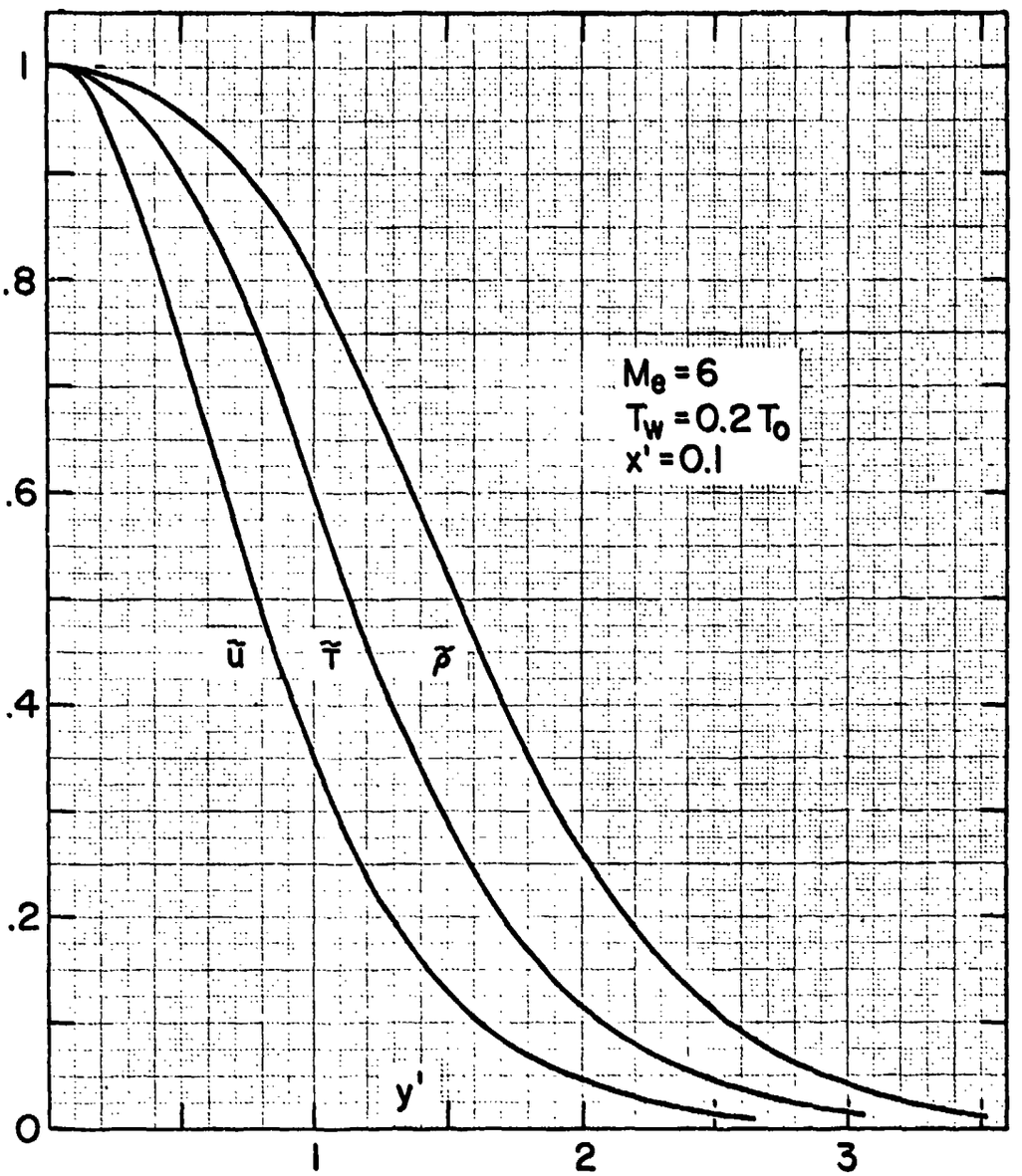

Figure 15: Typical profiles for a non-equilibrium symmetric wake.

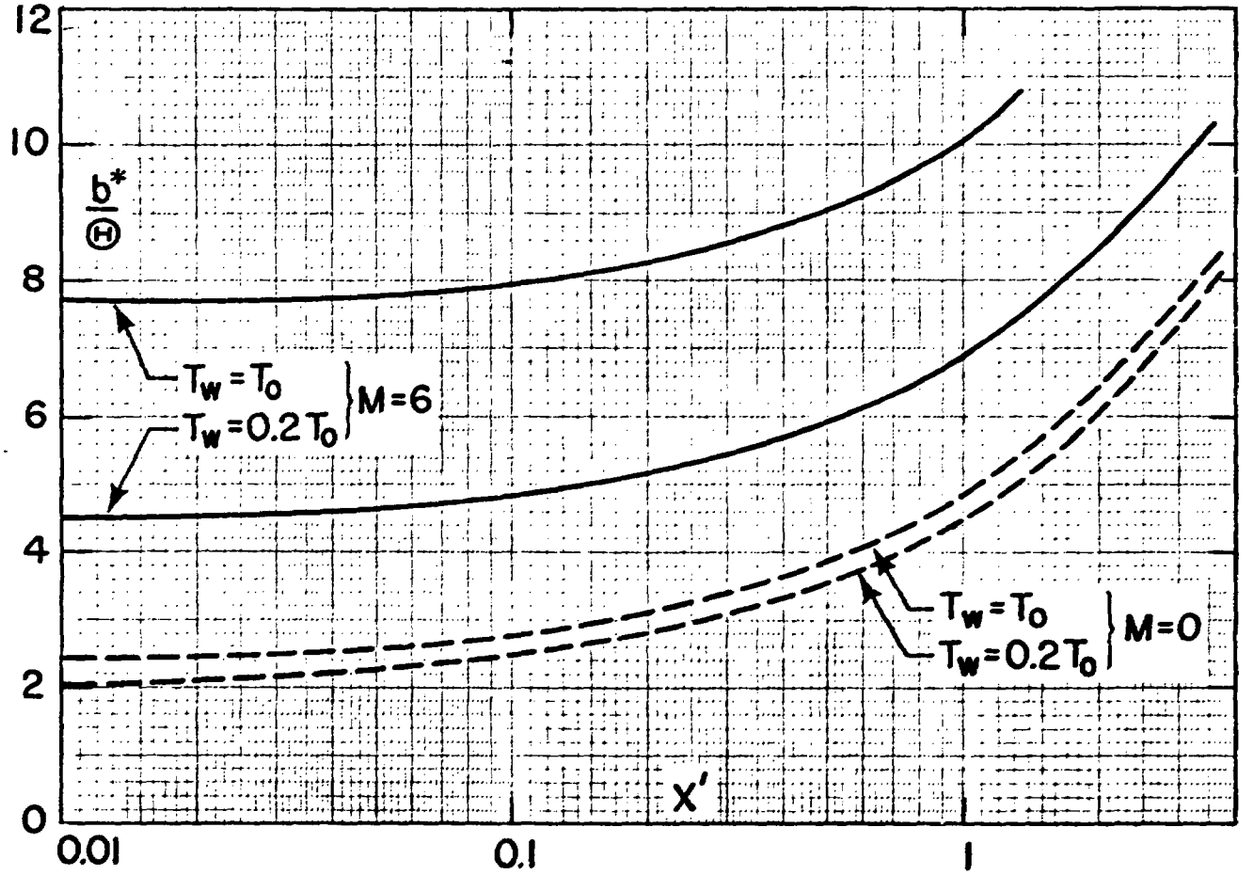

Figure 16: Typical physical velocity half-thickness for the symmetric wake.

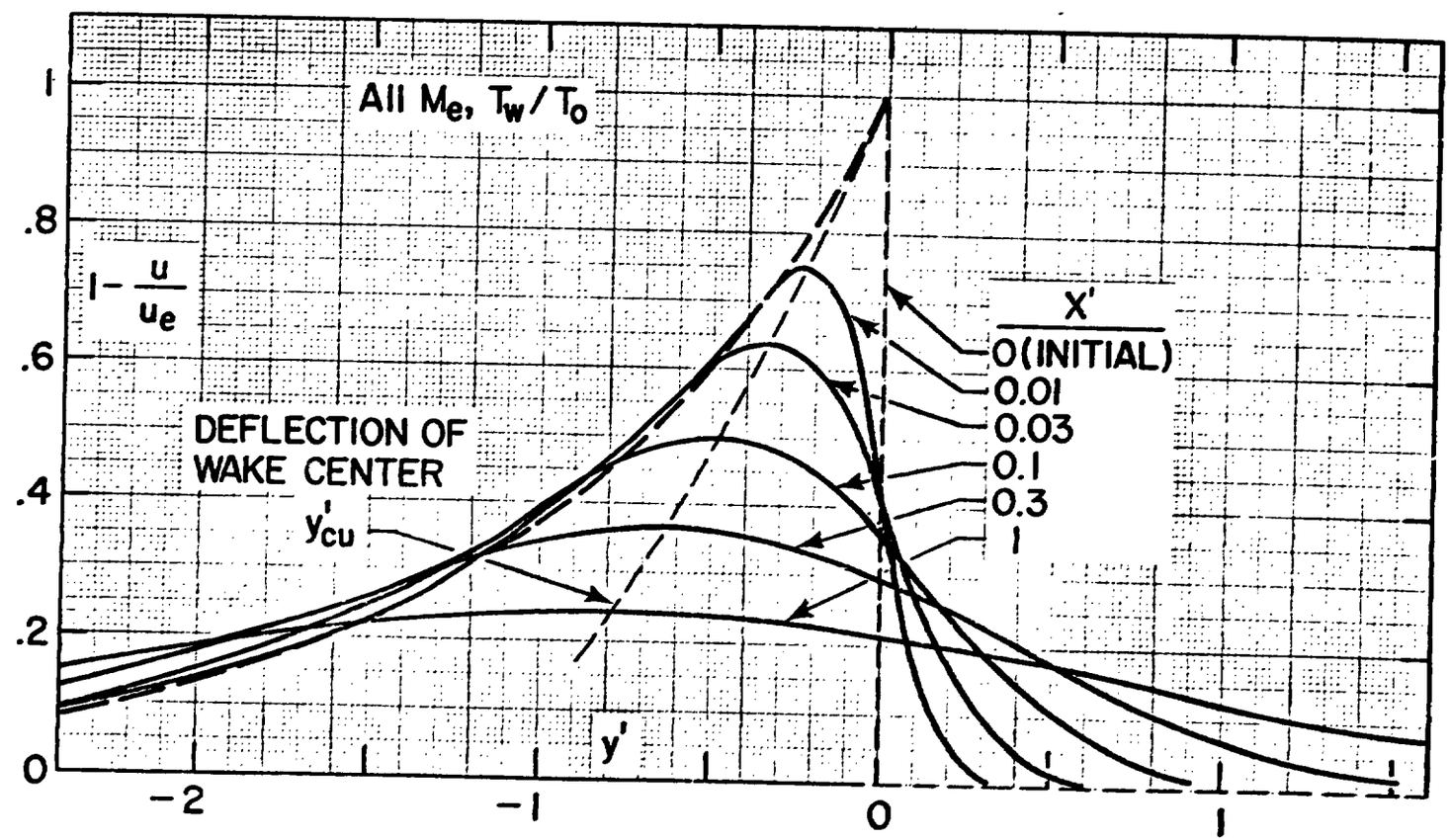

Figure 17: Development of the velocity variation for the asymmetric wake past the T.E.

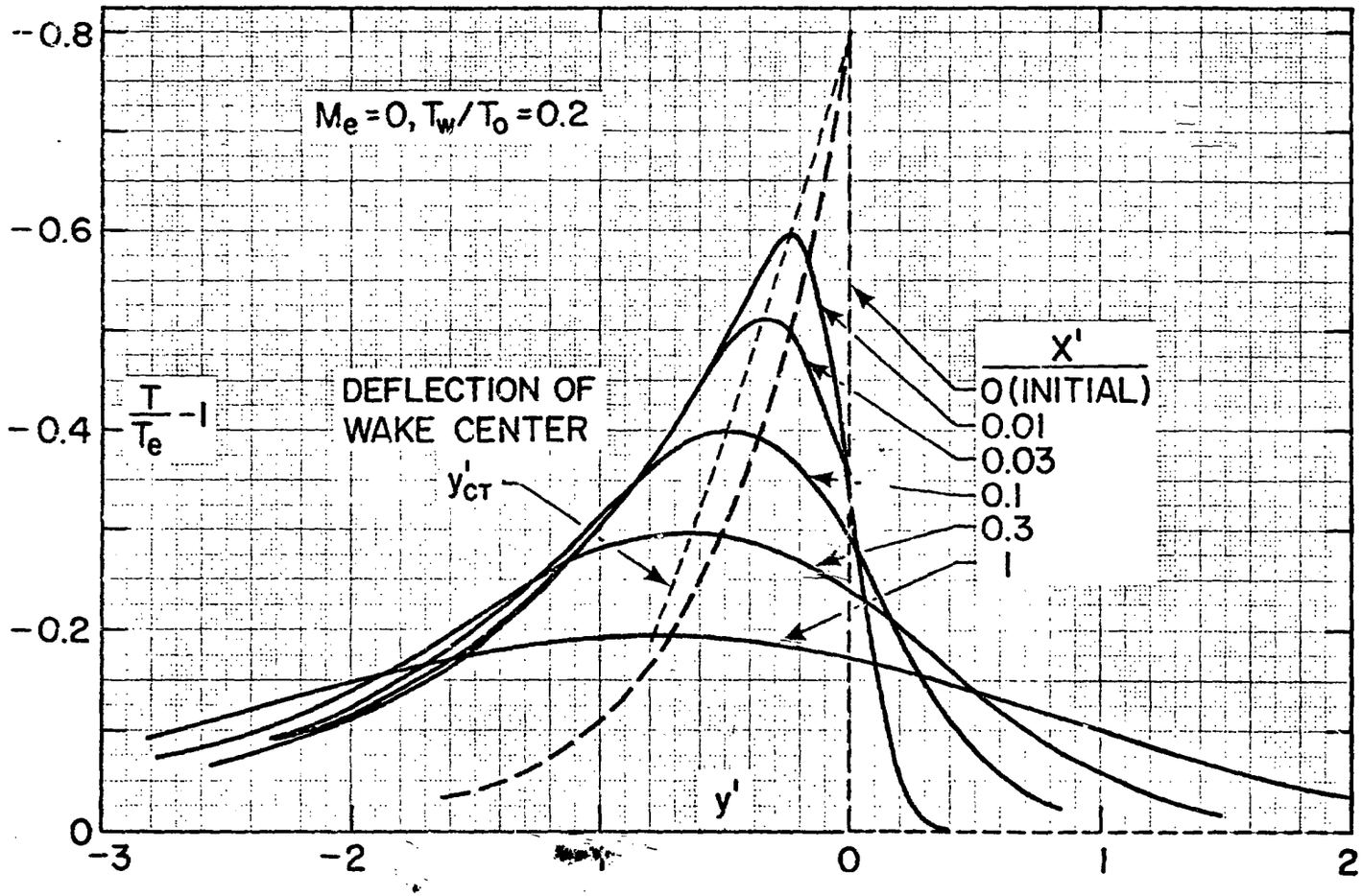

Figure 18: Temperature development of the low-speed, cooled asymmetric wake past the T.E.

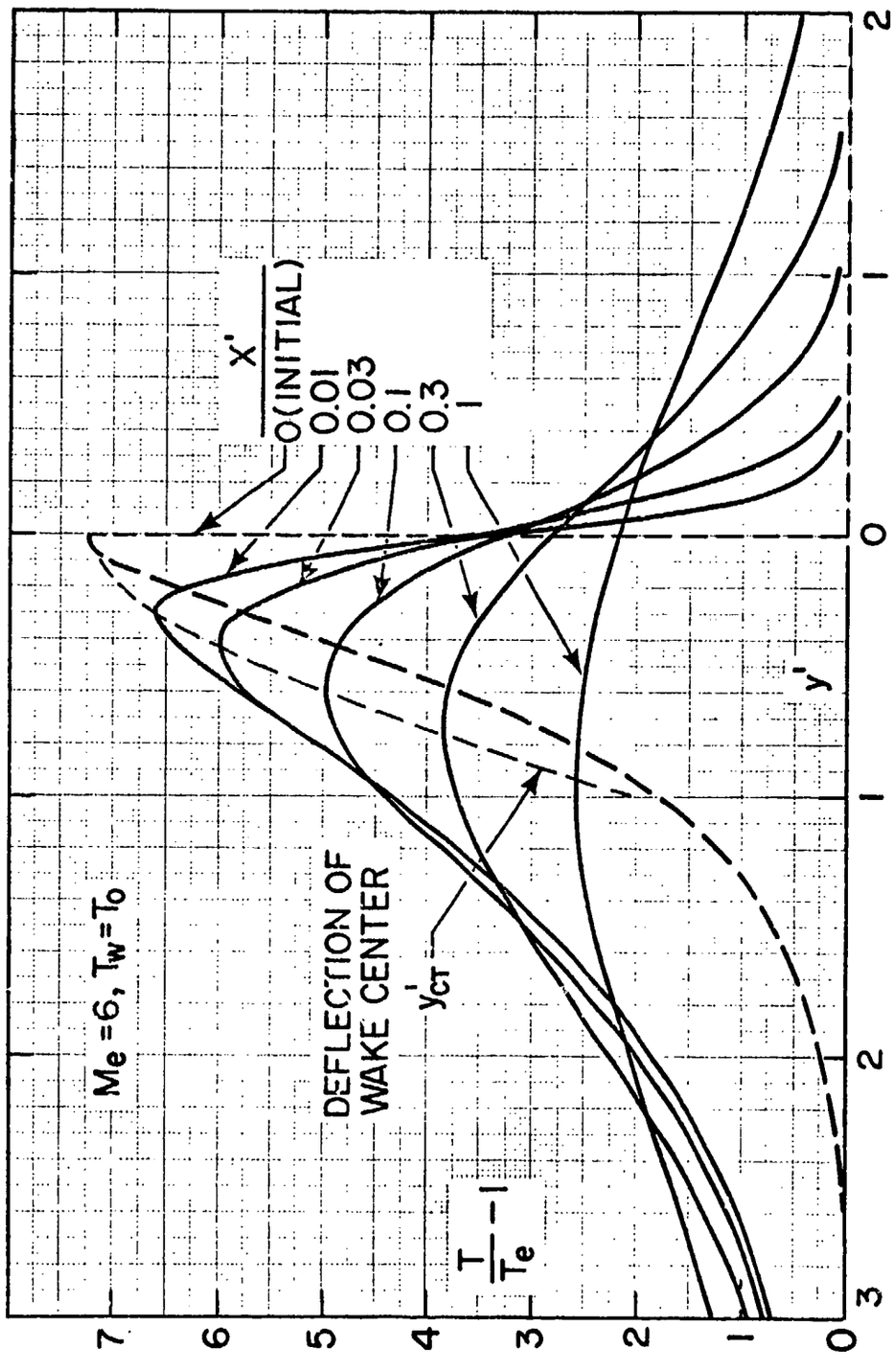

Figure 19: Temperature development of the hypersonic adiabatic asymmetric wake past the T.E.

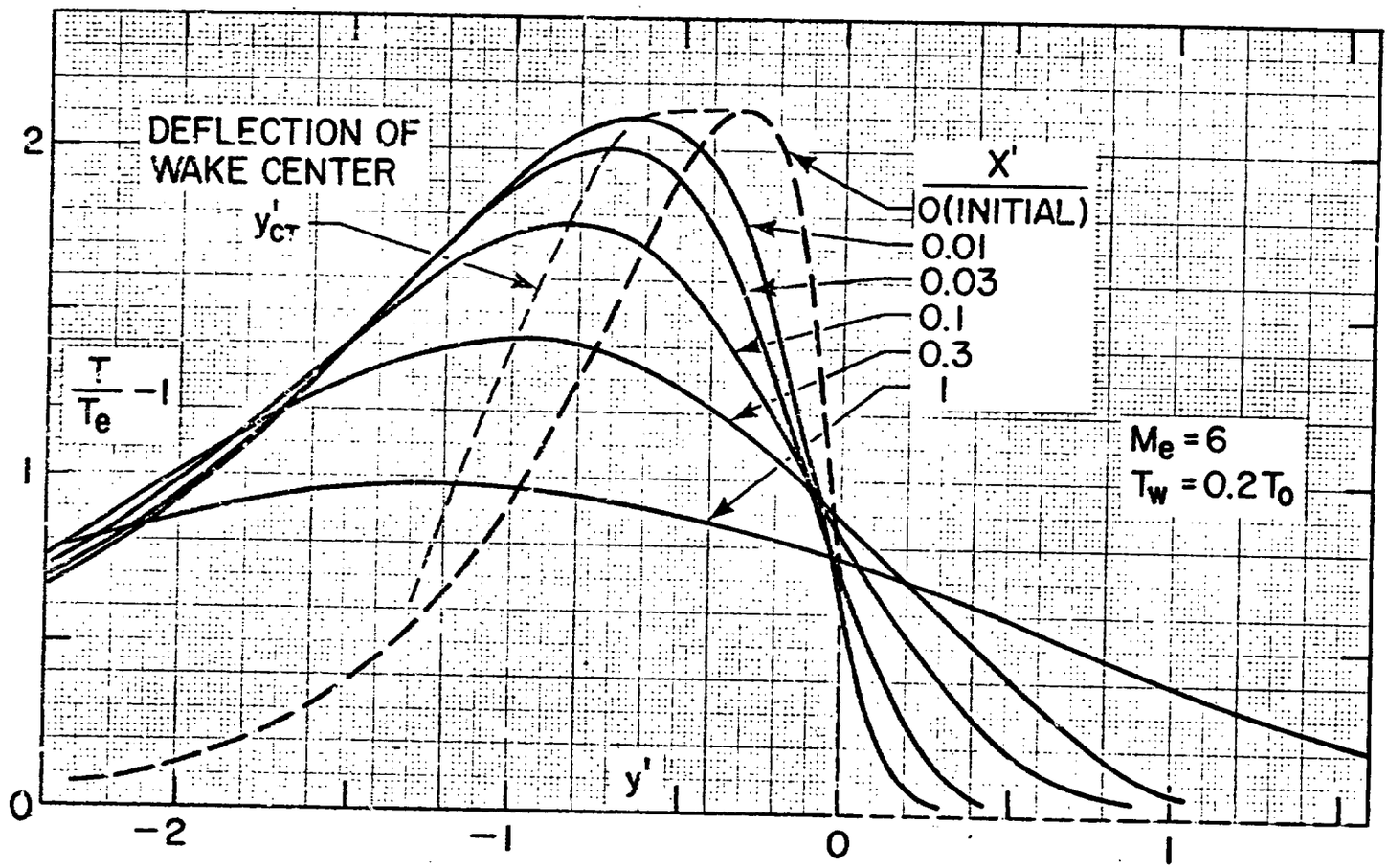

Figure 20: Temperature development of the hypersonic cooled asymmetric wake past the T.E.

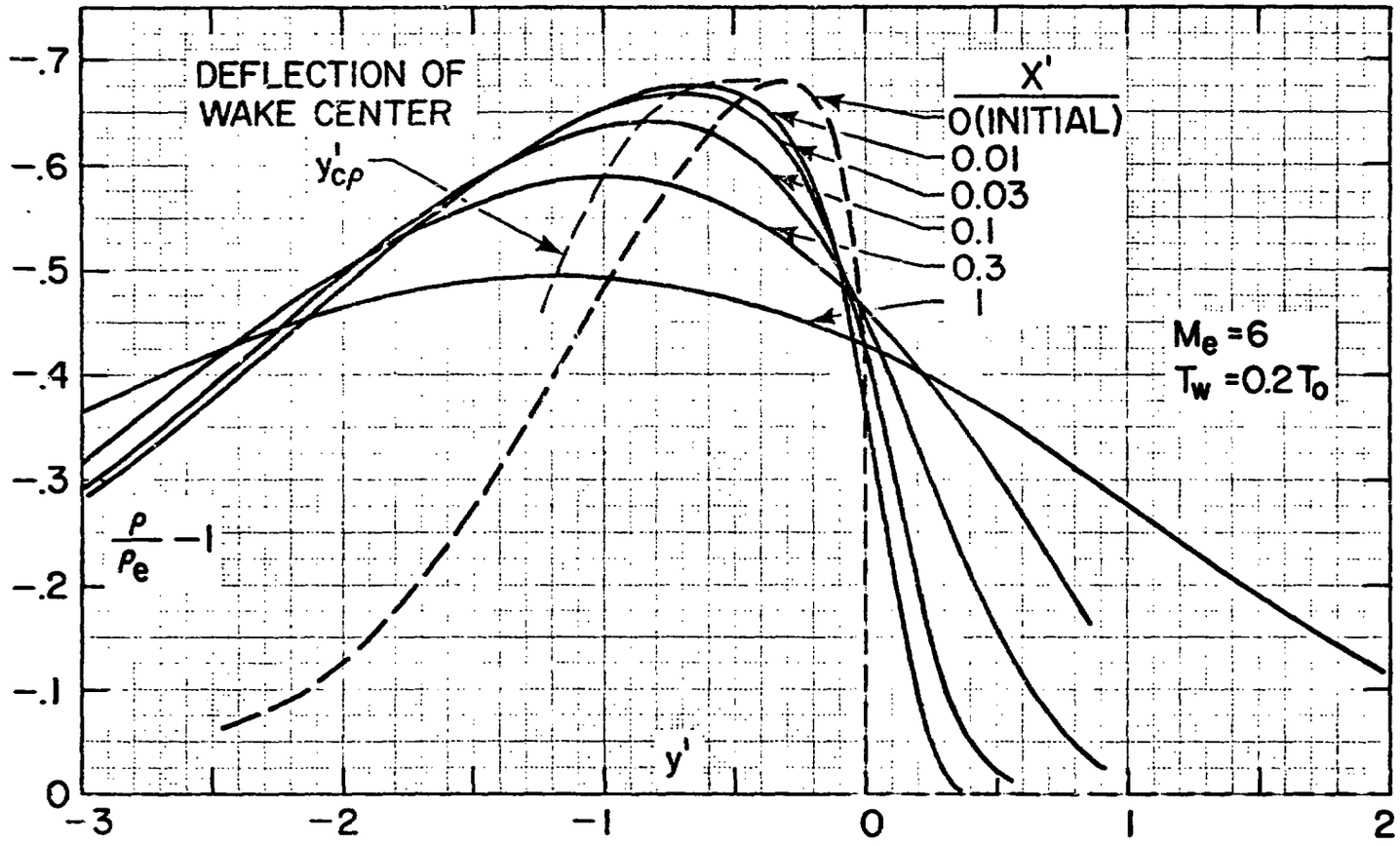

Figure 21: Density development of the hypersonic, cooled asymmetric wake past the T.E.

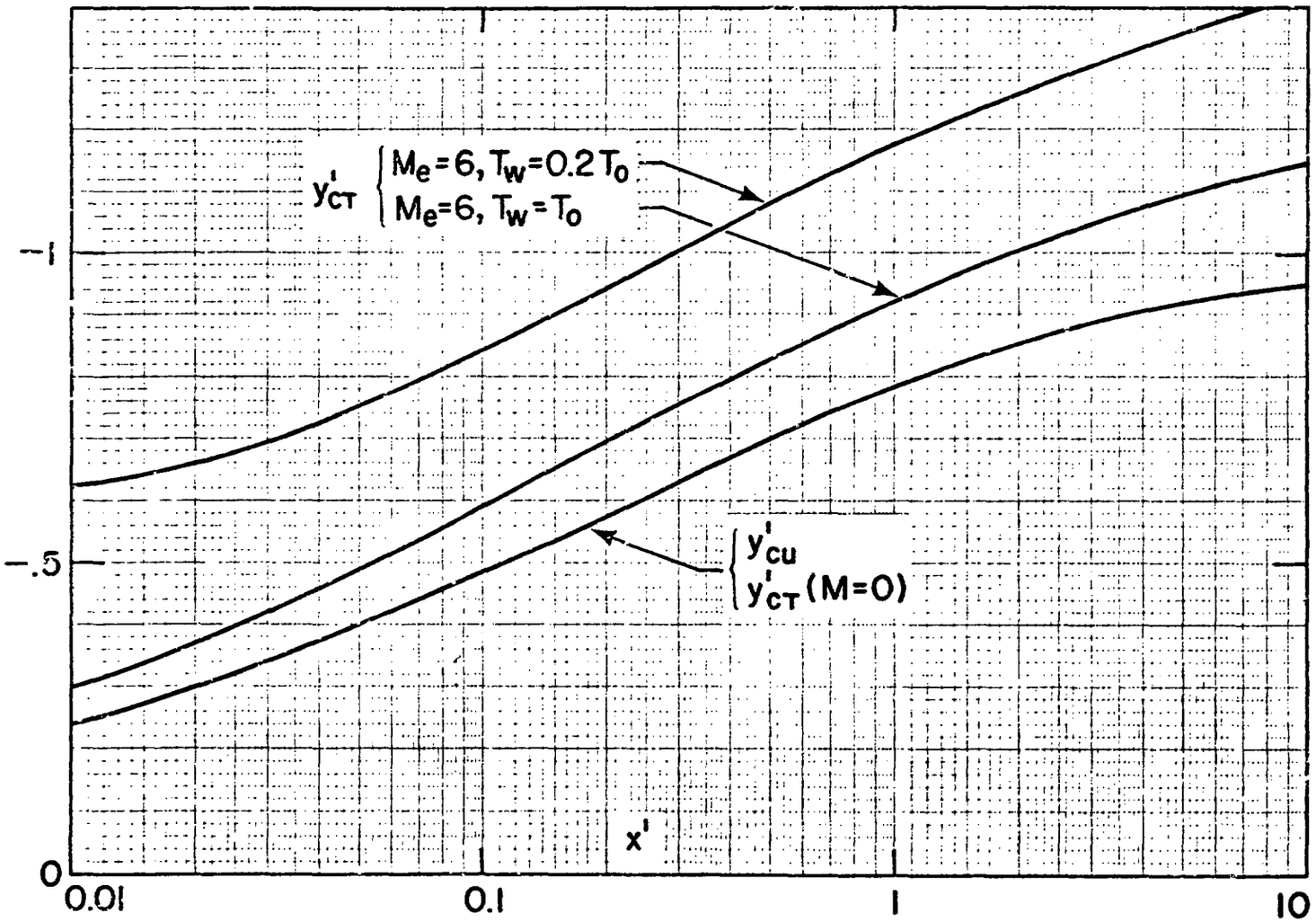

Figure 22: Typical deflection of the asymmetric wake centers (compressible-transformed coordinate).

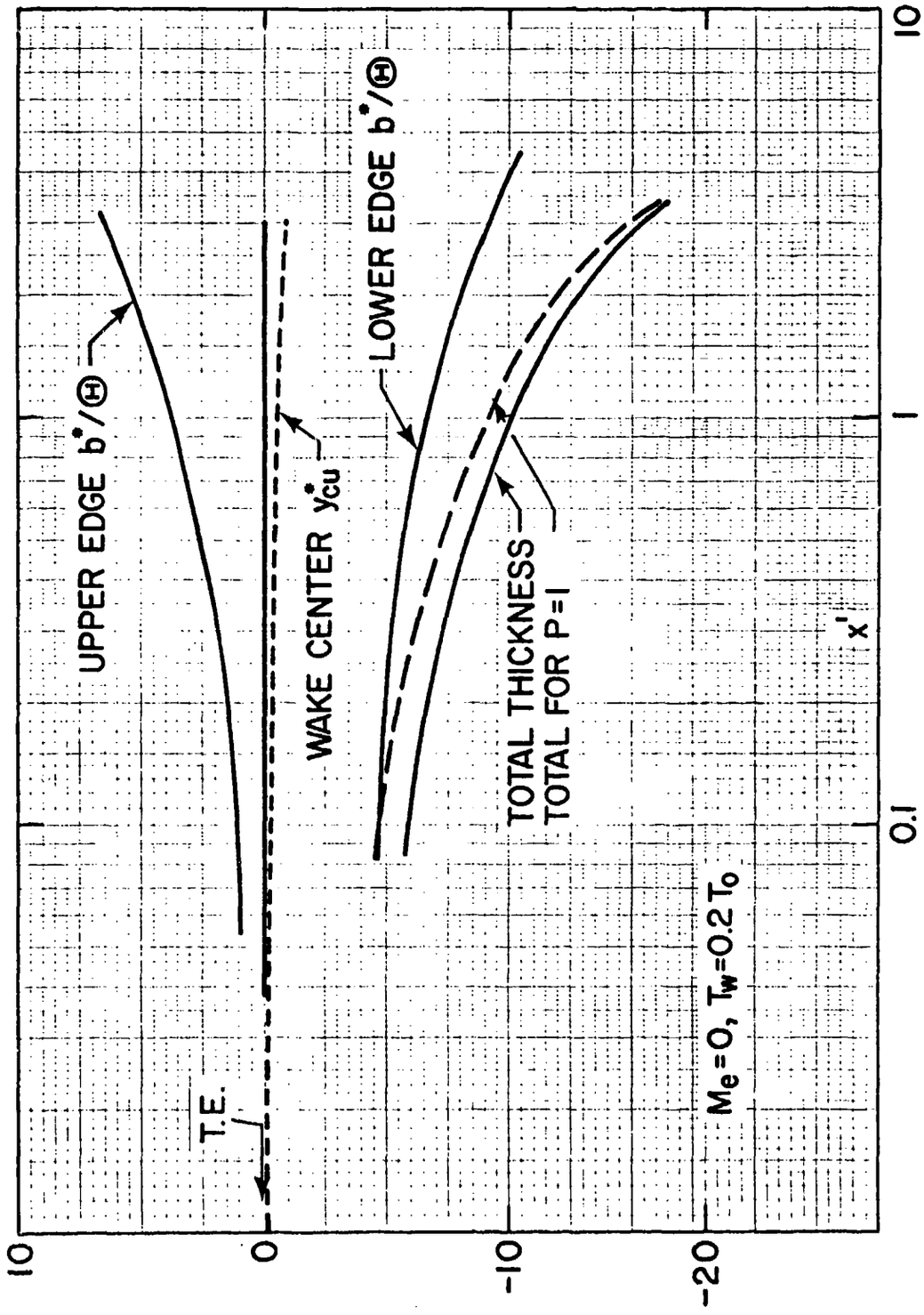

Figure 23: "Map" of the low-speed, cooled asymmetric wake.

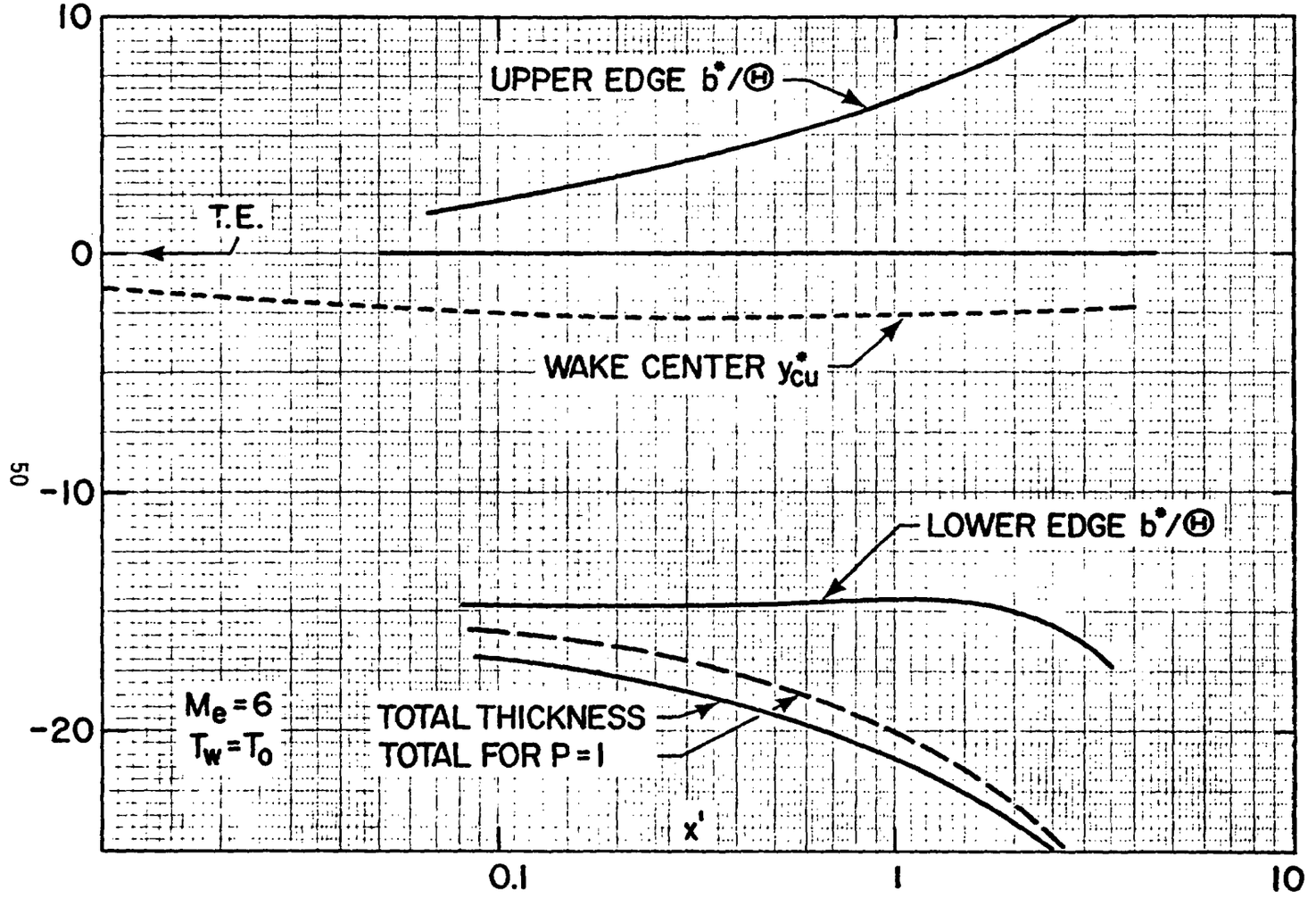

Figure 24: "Map" of the hypersonic adiabatic symmetric wake.

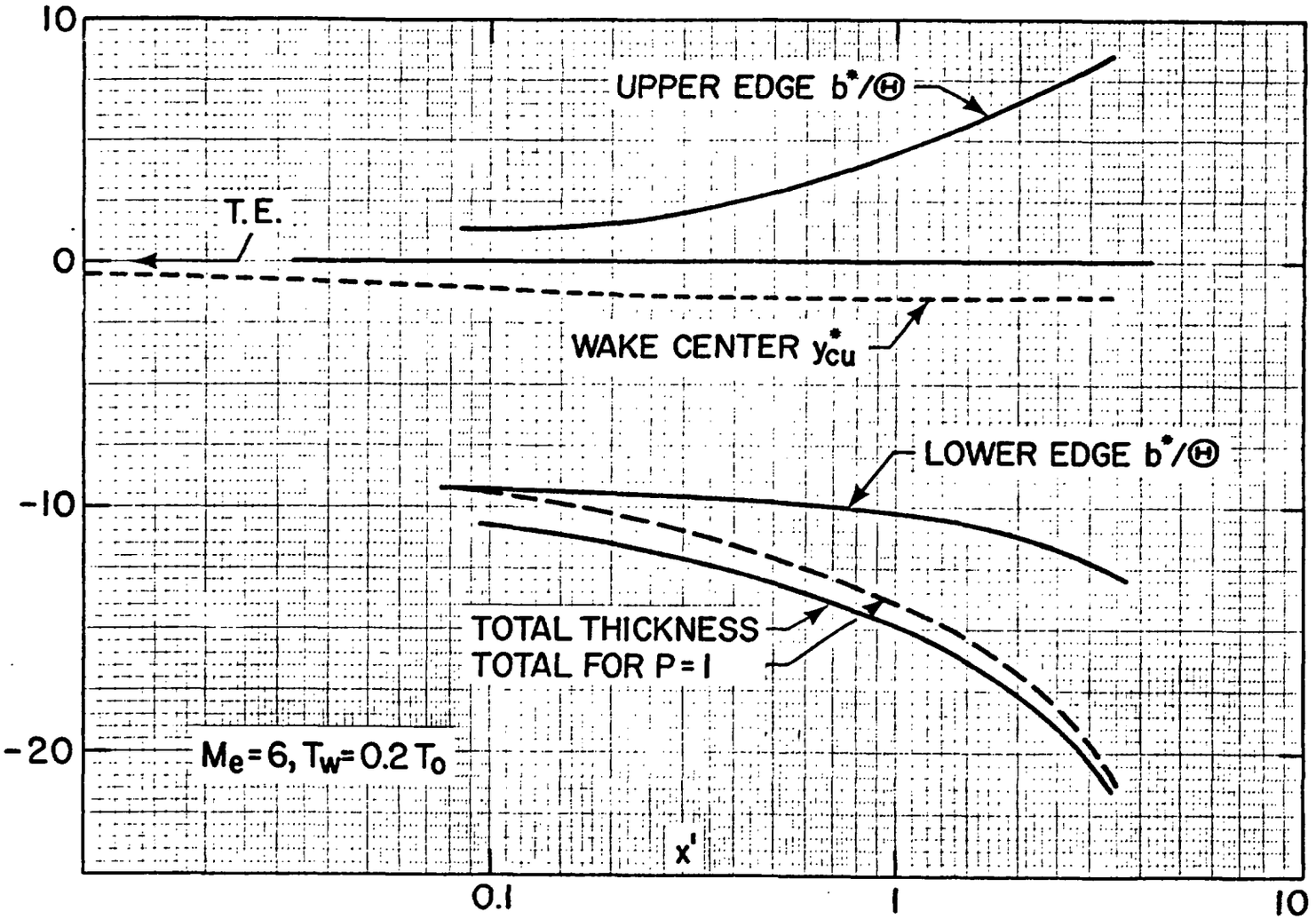

Figure 25: "Map" of the hypersonic cooled asymmetric wake.

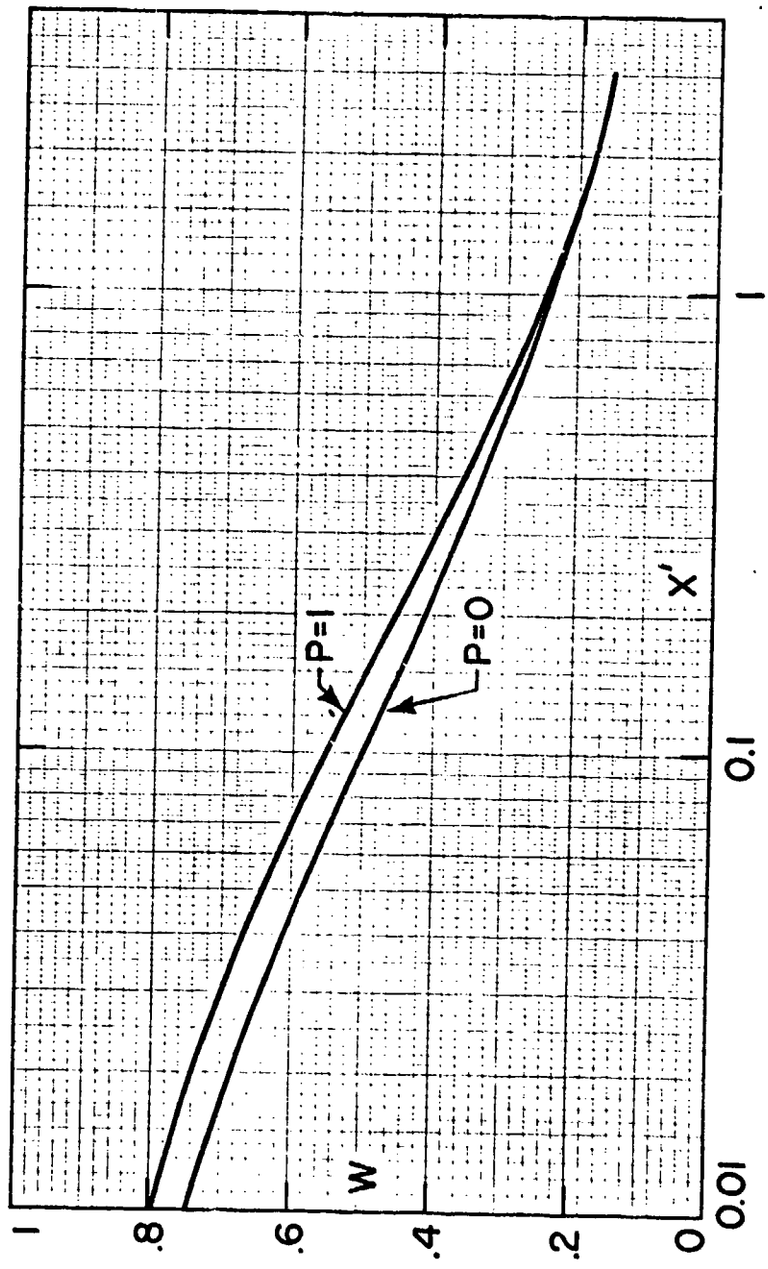

Figure 26: Effect of asymmetry on the velocity defect.

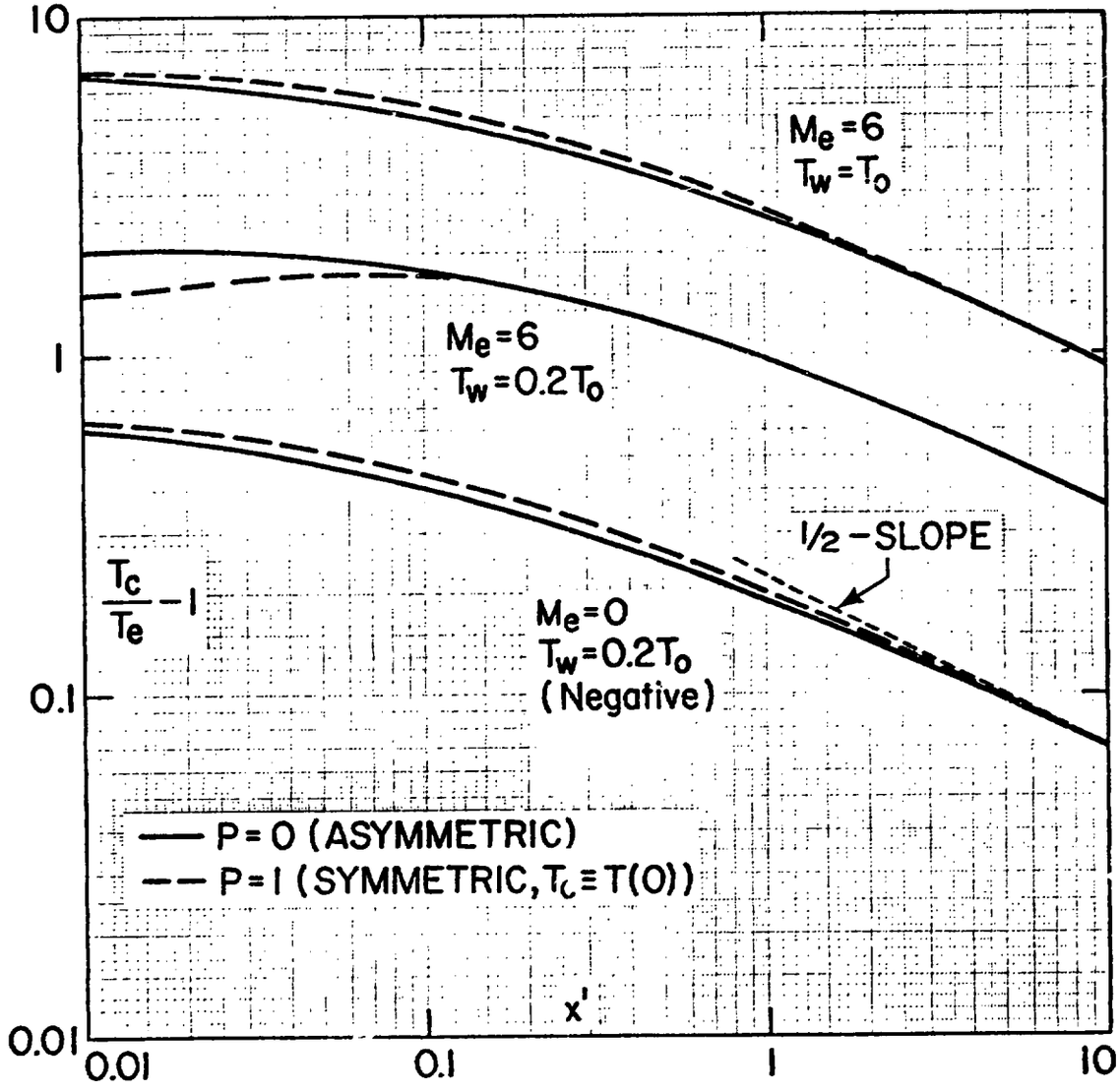

Figure 27: Effect of asymmetry on the temperature defect.

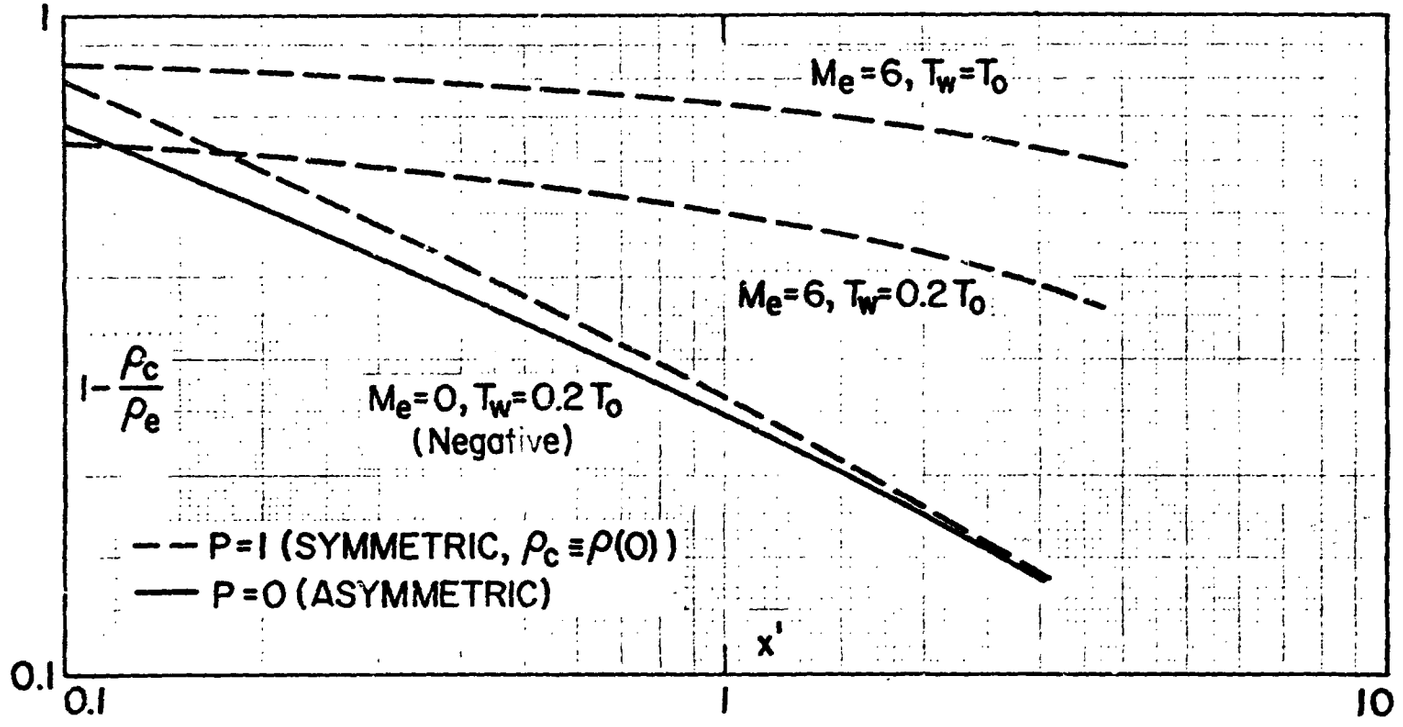

Figure 28: Effect of asymmetry on the density defect.

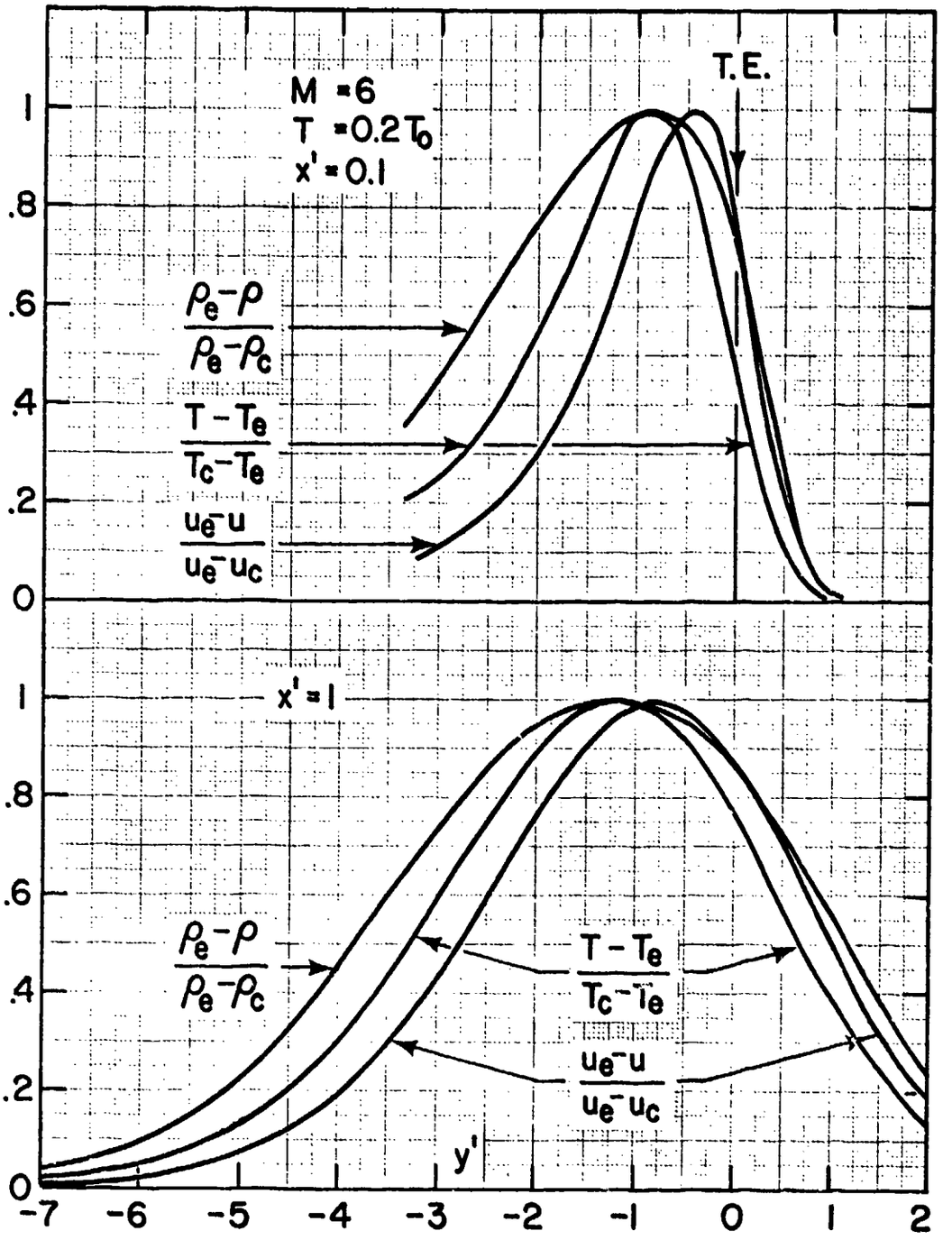

Figure 29: Comparison of normalized profiles for the hypersonic, cooled asymmetric wake in the non-equilibrium zone.

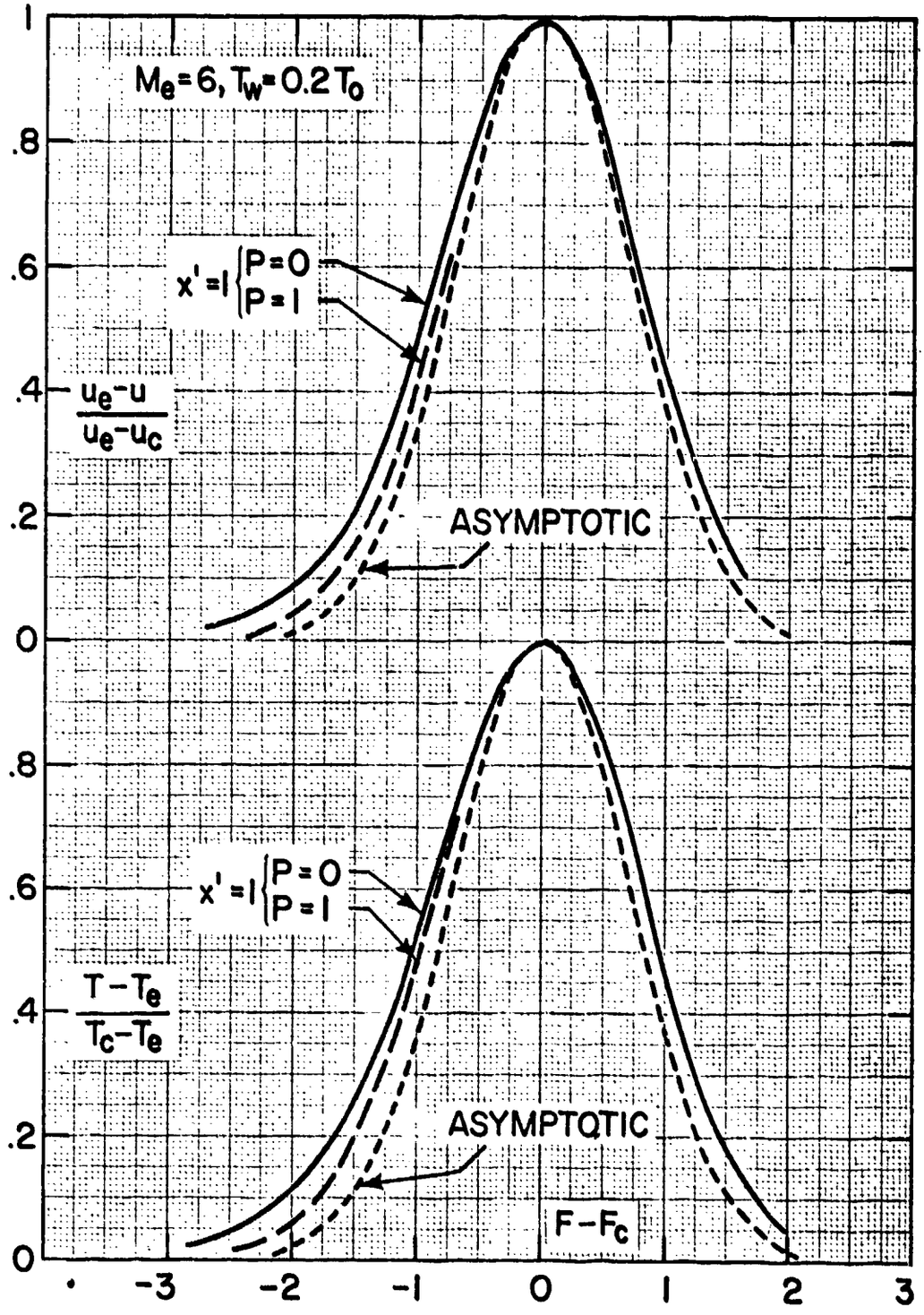

Figure 30: Decay of initial profile asymmetry in the hypersonic, cooled wake.

APPENDIX

COMPUTER PROGRAMS

All programs contained in this Appendix use the BASIC language.

The output symbols for each program, as they appear on the printout, are explained in terms of the symbols listed in the beginning of this report.

"WAKEFLOW2" PROGRAM

1. Purpose: To compute the defects for symmetric wakes as a function of x', with M_e and T_w/T_o as parameters.

2. Application Example

2.1 If the defects at a single x', M_e, T_w/T_o are desired:
Compute the defects at $M_e = 3$, $T_w/T_o = 1.5$, $x' = 0.6$.
Enter:

```
 30  LET T = 1.5
 40  LET M = 3
180  LET x = 0.6
410
460
470
```

2.2 If the defects at a single M_e, T_w/T_o but a series of x' are desired.
Compute the defects for the above example but for x' intervals of 0.05 from 0 to 0.8.
Enter:

```
 30  LET T = 1.5
 40  LET M = 3
180  FOR x = 0 TO 0.8 STEP 0.05
460
470
```

2.3 If one needs the defects for a series of x' at each of a series of M_e, and additionally for a series of T_w/To:
Compute the defects for $M_e = 0, 1, 2 \ldots 5$, and $T_w/T_o = 0.5$, 1, 1.5, each for x' from 0 to 2 in steps of 0.2.
Enter:

```
 30  FOR T = 0.5 TO 1.5 STEP 0.5
 40  FOR M = 0 TO 5 STEP 1
180  FOR x = 0 TO 2 STEP 0.1
```

3. Explanation of Output Symbols

Printout Symbol	Explanation
B	B
C	C
TO/TE-1	t
TO-TE/TW-TE	t′
1-RO/RE	r
RE-RO/RE-RW	$\bar{r}$
W	w
M(O)	M(O)
TOO-TOE/TOE	H
TOO-TOE/TW-TOE	$\bar{H}$

"WAKEFLO2" LISTING

```
10 REM WAKEFLO2
20 DIM X(40),X1(40),Y(40),W(40),X2(40),H(40),F(40),Z(40)
25 DIM H1(40),R(40),R1(40)
27 DIM M1(40),M2(40),M3(40)
30 FOR T=.2 TO 1.8 STEP .4
40 FOR M=0 TO 5 STEP 1
50 PRINT "SYMMETRIC WAKE DEFECTS"
60 PRINT "FOR TW/T0=";T
70 PRINT "AND MACH NO=";M
90 PRINT
100 LET B=.2*(M^2)*(T+1)+T-1
110 LET C=-.2*(M^2)
120 PRINT "THE CONSTANT B=";B
130 PRINT "THE CONSTANT C=";C
150 PRINT
160 PRINT "X","T0/TE-1","T0-TE/TW-TE","1-R0/RE","RE-R0/RE-RW"
165 PRINT TAB(6),"W","M(0)","T00-T0E/T0E","T00-T0E/TW-T0E"
170 PRINT
180 FOR X=0 TO 3 STEP .3
190 LET P=.327591
200 LET A1=.2548295924
210 LET A2=-.2844967360000001
220 LET A3=1.421413741
230 LET A4=-1.453152027
240 LET A5=1.061405429
250 LET X1=2*SQR(X)
260 LET D=1/(1+P*X1)
270 LET Y=(A1*D+A2*(D^2)+A3*(D^3)+A4*(D^4)+A5*(D^5))*EXP(-(X1^2))
280 LET W=(EXP(4*X))*Y
290 LET X2=2*X1
300 LET F=1/(1+P*X2)
310 LET Z=(A1*F+A2*(F^2)+A3*(F^3)+A4*(F^4)+A5*(F^5))*EXP(-(X2^2))
320 LET H=B*W+C*EXP(16*X)*Z
330 LET H1=H/(B+C)
340 LET R=H/(H+1)
350 LET R1=R*(1+1/(B+C))
360 LET M1=M*(1-W)/SQR(1+H)
370 LET H2=((H+1)*(1+.2*(M1^2))/(1+.2*(M^2)))-1
380 LET H3=H2/(T-1)
390 PRINT X,H,H1,R,R1
400 PRINT TAB(6),W,M1,H2,H3
410 NEXT X
420 PRINT
430 PRINT
460 NEXT M
470 NEXT T
500 END
```

"WAKEFLO2" OUTPUT

SYMMETRIC WAKE DEFECTS
FOR TW/T0= .5
AND MACH NO= 2

THE CONSTANT B= .7
THE CONSTANT C=-.8

X'	T0/TE-1 W	T0-TE/TW-TE M(0)	1-R0/RE T00-T0E/T0E	RE-R0/RE-RW T00-T0E/TW-T0E
0	-.1	1	-.111111	1
	1	0	-.5	1
.2	.0967988	-.967988	.0382557	-.794302
	.458246	1.03459	-.260224	.520449
.4	.0883864	-.883865	.0812087	-.730879
	.364732	1.21785	-.215979	.431957
.6	.0804491	-.804491	.074459	-.670131
	.313716	1.32048	-.190423	.380847
.8	.0740563	-.740563	.0689501	-.629551
	.279967	1.38953	-.172881	.345762
1	.0688763	-.688763	.064438	-.579943
	.255403	1.44042	-.159769	.319537
1.2	.0645929	-.645929	.0606736	-.546064
	.236448	1.48005	-.149444	.298887
1.4	.0609823	-.609823	.0574772	-.517295
	.221232	1.51211	-.141019	.282037
1.6	.0578878	-.578878	.0547201	-.492481
	.208658	1.53877	-.133963	.267926
1.8	.0551987	-.551988	.0523112	-.470801
	.198037	1.56141	-.127937	.255873

"WAKEFLO3" PROGRAM

1. Purpose: To compute the lateral profiles of symmetric wakes at a fixed x', M_e, T_w/T_o, as a function of y'.

2. Application Example

Compute the profiles for $x' = 0.25$, $M_e = 1$ and $T_w/T_o = 1$, for y' intervals of 0.15 from 0 to 3.

Enter:

```
30  LET M = 1
40  LET T = 1
50  LET x = 0.25
360  FOR V = 0 TO 3 STEP 0.15
```

3. Explanation of Output Symbols

Printout Symbol	Explanation
Y'	y'
Y'/2SQRX'	F
UTILDA	$\tilde{u}$
TTILDA	$\tilde{T}$
RHOTILDA	
M	$\tilde{M}$
TOTILDA	$\tilde{H}$

"WAKEFLO3" LISTING

```
10 REM WAKEFLO3
15 DIM M1(20),H2(20),H3(20),H4(20)
20 DIM V(20),Y1(20),Y2(20),R(20),Y3(20),Y4(20),R1(20),U(20)
21 DIM R5(20)
30 LET M=1
40 LET T=1
50 LET X=.25
60 PRINT "SYMMETRIC WAKE PROFILES"
70 PRINT "-------------------------"
80 PRINT
90 PRINT "FOR X'=";X
100 PRINT "AND M=";M
110 PRINT "AND TW/T0=";T
120 PRINT
130 LET B=.2*(M^2)*(T+1)+T-1
140 LET C=-.2*(M^2)
150 PRINT "COMPUTED CONSTANT B=";B
160 PRINT "COMPUTED CONSTANT C=";C
170 LET P=.327591
180 LET A1=.254829592#
190 LET A2=-.28449673600000001#
200 LET A3=1.421413741#
210 LET A4=-1.453152027#
220 LET A5=1.061405429#
230 LET X1=2*SQR(X)
240 LET D=1/(1+P*X1)
250 LET Y=(A1*D+A2*(D^2)+A3*(D^3)+A4*(D^4)+A5*(D^5))*EXP(-(X1^2))
260 LET W=Y*EXP(4*X)
270 PRINT "COMPUTED W=";W
280 LET X2=2*X1
290 LET F=1/(1+P*X2)
300 LET Z=(A1*F+A2*(F^2)+A3*(F^3)+A4*(F^4)+A5*(F^5))*EXP(-(X2^2))
310 LET H=B*W+C*EXP(16*X)*Z
320 PRINT "COMPUTED H=T(0)/TE - 1=";H
325 PRINT "COMPUTED DEFECT H'=(T(0)-TE/TW-TE)=";H/(B+C)
330 PRINT
340 PRINT "Y'","Y'/2SQRX'","UTILDA","TTILDA","RHOTILDA"
345 PRINT TAB(8),"M","T0TILDA"
350 PRINT
360 FOR V=0 TO 3 STEP .15
370 LET Y1=V/X1+X1
380 LET Y2=1/(1+P*Y1)
390 LET R=(A1*Y2+A2*(Y2^2)+A3*(Y2^3)+A4*(Y2^4)+A5*(Y2^5))*EXP(-(Y1^2))
400 LET Y3=V/X1-X1
405 IF Y3<0 GOTO 422
410 LET Y4=1/(1+P*Y3)
420 LET R1=1-(A1*Y4+A2*(Y4^2)+A3*(Y4^3)+A4*(Y4^4)+A5*(Y4^5))*EXP(-(Y3^2))
421 GOTO 430
422 LET Y3=X1-V/X1
424 LET Y4=1/(1+P*Y3)
```

"WAKEFLO3" LISTING (CONT'D)

```
426 LET R1=(A1*Y4+A2*(Y4^2)+A3*(Y4^3)+A4*(Y4^4)+A5*(Y4^5))*EXP(-(Y3^2))
428 LET U=.5*(R*EXP(4*X+2*V)+R1*EXP(4*X-2*V))/W
429 GOTO 440
430 LET U=.5*(R*EXP(4*X+2*V)+(1+R1)*EXP(4*X-2*V))/W
440 LET Y5=2*X1+V/X1
450 LET Y6=1/(1+P*Y5)
460 LET R2=(A1*Y6+A2*(Y6^2)+A3*(Y6^3)+A4*(Y6^4)+A5*(Y6^5))*EXP(-(Y5^2))
470 LET Y7=X1-V/X1
480 IF Y7<0 GOTO 520
490 LET Y8=1/(1+P*Y7)
500 LET R3=(A1*Y8+A2*(Y8^2)+A3*(Y8^3)+A4*(Y8^4)+A5*(Y8^5))*EXP(-(Y7^2))
510 GOTO 550
520 LET Y7=V/X1-X1
530 LET Y8=1/(1+P*Y7)
540 LET R3=2-(A1*Y8+A2*(Y8^2)+A3*(Y8^3)+A4*(Y8^4)+A5*(Y8^5))*EXP(-(Y7^2))
550 LET Y9=2*X1-V/X1
560 IF Y9<0 GOTO 600
570 LET F1=1/(1+P*Y9)
580 LET R4=(A1*F1+A2*(F1^2)+A3*(F1^3)+A4*(F1^4)+A5*(F1^5))*EXP(-(Y9^2))
590 GOTO 630
600 LET Y9=V/X1-2*X1
610 LET F1=1/(1+P*Y9)
620 LET R4=2-(A1*F1+A2*(F1^2)+A3*(F1^3)+A4*(F1^4)+A5*(F1^5))*EXP(-(Y9^2))
630 LET T1=.5*(B*(EXP(4*X-2*V)*R3+EXP(4*X+2*V)*R))
633 LET T2=.5*(C*(EXP(16*X-4*V)*R4+EXP(16*X+4*V)*R2))
637 LET T3=T1+T2
640 LET T4=T3/H
645 LET R5=(T4*(H+1))/(T4*H+1)
646 LET M1=M*(1-U*W)/SQR(1+T4*H)
647 LET H2=((H+1)*(1+.2*(M1^2))/(1+.2*(M^2)))-1
648 LET H3=(1+T4*H)*(1+.2*(M1^2))/(1+.2*(M^2))-1
649 LET H4=H3/H2
650 PRINT V,V/X1,U,T4,R5
655 PRINT TAB(8),M1,H4
660 NEXT V
700 END
```

"WAKEFL03" OUTPUT

SYMMETRIC WAKE PROFILES

FOR X'= .25
AND M= 1
AND TW/T0= 1

COMPUTED CONSTANT B= .4
COMPUTED CONSTANT C=-.2
COMPUTED W= .427584
COMPUTED H=T(0)/TE - 1= .119953
COMPUTED DEFECT H'=(T(0)-TE/TW-TE)= .599765

Y'	Y'/2SQRX' M	UTILDA T0TILDA	TTILDA	RHOTILDA
0	0	1	1	1
	.540894	1		
.15	.15	.985738	.987599	.988913
	.54702	1.12106		
.3	.3	.944288	.951407	.956384
	.564875	1.7231		
.45	.45	.879449	.894323	.904561
	.592966	11.5166		
.6	.6	.796859	.820713	.836781
	.629039	-1.70369		
.75	.75	.703141	.73582	.757247
	.670389	-.675035		
.9	.9	.604977	.645114	.670604
	.714203	-.371414		
1.05	1.05	.508323	.553693	.58149
	.757886	-.227826		
1.2	1.2	.417857	.465832	.4941
	.799303	-.145981		
1.35	1.35	.336733	.384717	.411859
	.836925	-.0949776		
1.5	1.5	.266615	.312385	.337221
	.869852	-.0618271		
1.65	1.65	.207897	.249804	.271629
	.897756	-.03993		
1.8	1.8	.160037	.197067	.215609
	.920752	-.0254572		
1.95	1.95	.121906	.153633	.168949
	.93926	-.0159722		
2.1	2.1	.0920926	.118563	.130922
	.953864	-9.84869E-03		
2.25	2.25	.0691332	.0907185	.100507
	.965202	-5.96667E-03		
2.4	2.4	.0516595	.0689246	.0765593
	.973894	-3.55195E-03		
2.55	2.55	.0384782	.0520665	.05795
	.98049	-2.08039E-03		
2.7	2.7	.0285984	.0391517	.0436431
	.98546	-1.20079E-03		
2.85	2.85	.0212262	.0293344	.032738
	.989185	-6.84796E-04		

"WAKEFLO4" PROGRAM

1. Purpose: To compute the physical velocity half-thickness (defined at $\tilde{u} = 0.01$) for a symmetric wake, given M_e, T_w/T_o, x', and $y'(\tilde{u} = 0.01)$. The latter is found by first using the WAKEFLO3 program.

2. Application Example

Compute the half thickness for $M_e = 5$, $T_w/T_o = 1$, $x' = 0.1$; for this case, WAKEFLO3 gives $y'(\tilde{u} = 0.01) = 2.7$.

Enter:

```
30  LET M = 5
40  LET T = 1
50  LET X = 0.1
360  LET V = 2.7
```

"WAKEFLO4" LISTING

```
10 REM WAKEFLO4
20 DIM V(40),Y1(40),Y2(40),R(40),Y3(40),Y4(40),R1(40),U(40)
21 DIM R5(40),V1(40),R6(40),V2(40)
30 LET M=5
40 LET T=1
50 LET X=.1
60 PRINT "PHYSICAL VELOCITY HALF-THICKNESS COMPUTATION (UTILDA=0.01)"
70 PRINT "FOR SYMMETRIC WAKES"
75 PRINT "-----------------------------------------"
80 PRINT
90 PRINT "FOR X'=";X
100 PRINT "AND M=";M
110 PRINT "AND TW/T0=";T
120 PRINT
130 LET B=.2*(M^2)*(T+1)+T-1
140 LET C=-.2*(M^2)
170 LET P=.327591
180 LET A1=.254829592#
190 LET A2=-.28449673600000001#
200 LET A3=1.421413741#
210 LET A4=-1.453152027#
220 LET A5=1.061405429#
230 LET X1=2*SQR(X)
240 LET D=1/(1+P*X1)
250 LET Y=(A1*D+A2*(D^2)+A3*(D^3)+A4*(D^4)+A5*(D^5))*EXP(-(X1^2))
260 LET W=Y*EXP(4*X)
280 LET X2=2*X1
290 LET F=1/(1+P*X2)
300 LET Z=(A1*F+A2*(F^2)+A3*(F^3)+A4*(F^4)+A5*(F^5))*EXP(-(X2^2))
310 LET H=B*W+C*EXP(16*X)*Z
360 LET V=2.7
650 FOR I=1 TO 40
660 LET V1(I)=I*V/40
665 LET V1=V1(I)
1370 LET Y1=V1/X1+X1
1380 LET Y2=1/(1+P*Y1)
1390 LET R=(A1*Y2+A2*(Y2^2)+A3*(Y2^3)+A4*(Y2^4)+A5*(Y2^5))*EXP(-(Y1^2))
1400 LET Y3=V1/X1-X1
1405 IF Y3<0 GOTO 1422
1410 LET Y4=1/(1+P*Y3)
1420 LET R1=1-(A1*Y4+A2*(Y4^2)+A3*(Y4^3)+A4*(Y4^4)+A5*(Y4^5))*EXP(-(Y3^2))
1421 GOTO 1430
1422 LET Y3=X1-V1/X1
1424 LET Y4=1/(1+P*Y3)
1426 LET R1=(A1*Y4+A2*(Y4^2)+A3*(Y4^3)+A4*(Y4^4)+A5*(Y4^5))*EXP(-(Y3^2))
1428 LET U=.5*(R*EXP(4*X+2*V1)+R1*EXP(4*X-2*V1))/W
1429 GOTO 1440
1430 LET U=.5*(R*EXP(4*X+2*V1)+(1+R1)*EXP(4*X-2*V1))/W
1440 LET Y5=2*X1+V1/X1
```

"WAKEFLO4" LISTING (CONT'D)

```
1450 LET Y6=1/(1+P*Y5)
1460 LET R2=(A1*Y6+A2*(Y6^2)+A3*(Y6^3)+A4*(Y6^4)+A5*(Y6^5))*EXP(-(Y5^2))
1470 LET Y7=X1-V1/X1
1480 IF Y7<0 GOTO 1520
1490 LET Y8=1/(1+P*Y7)
1500 LET R3=(A1*Y8+A2*(Y8^2)+A3*(Y8^3)+A4*(Y8^4)+A5*(Y8^5))*EXP(-(Y7^2))
1510 GOTO 1550
1520 LET Y7=V1/X1-X1
1530 LET Y8=1/(1+P*Y7)
1540 LET R3=2-(A1*Y8+A2*(Y8^2)+A3*(Y8^3)+A4*(Y8^4)+A5*(Y8^5))*EXP(-(Y7^2))
1550 LET Y9=2*X1-V1/X1
1560 IF Y9<0 GOTO 1600
1570 LET F1=1/(1+P*Y9)
1580 LET R4=(A1*F1+A2*(F1^2)+A3*(F1^3)+A4*(F1^4)+A5*(F1^5))*EXP(-(Y9^2))
1590 GOTO 1630
1600 LET Y9=V1/X1-2*X1
1610 LET F1=1/(1+P*Y9)
1620 LET R4=2-(A1*F1+A2*(F1^2)+A3*(F1^3)+A4*(F1^4)+A5*(F1^5))*EXP(-(Y9^2))
1630 LET T1=.5*(B*(EXP(4*X-2*V1)*R3+EXP(4*X+2*V1)*R))
1633 LET T2=.5*(C*(EXP(16*X-4*V1)*R4+EXP(16*X+4*V1)*R2))
1637 LET T3=T1+T2
1640 LET T4=T3/H
1645 LET R5=(T4*(H+1))/(T4*H+1)
1650 LET R6=1+T3
1660 LET V2=V2+R6*V/40
1670 NEXT I
1800 PRINT "TRANSFORMED HALF THICKNESS (YTILDA/CAPTHETA)=";V
1810 PRINT "PHYSICAL HALF THICKNESS (Y/CAPTHETA)=";V2
2000 END
```

"WAKEFL04" OUTPUT

```
PHYSICAL VELOCITY HALF-THICKNESS COMPUTATION (UTILDA=0.01)
FOR SYMMETRIC WAKES
-------------------------------------------------

FOR X'= .1
AND M= 5
AND TW/T0= 1

TRANSFORMED HALF THICKNESS (YTILDA/CAPTHETA)= 2.7
PHYSICAL HALF THICKNESS (Y/CAPTHETA)= 6.29334
```

"WAKEFLO6" PROGRAM

1. Purpose: To compute the "profiles" for the completely asymmetric (P = 0) wake for a given x', M_e, and T_w/T_o, for intervals of y' over a specified range of y'.

2. Application Example

Compute the profiles for P = 0 and x' = 0.01, M_e = 1 and T_w/T_o = 1.01 in steps of y' = 0.3 over the range from y' = -3 to +3.

Enter:

```
20  LET X = 0.01
22  LET M = 1
24  LET T = 1.01
160  FOR Y = -3 to 3 STEP 0.3
```

3. Explanation of Output Symbols

Printout Symbol	Explanation
Y'	y'
Y'/2SQR(X')	F
1 - U/UE	1 - u/ue
T/TE - 1	T/T_e - 1
R/RE - 1	ρ/ρ_e - 1
M	M
TO/TOE - 1	T_o/T_{oe} - 1

"WAKEFLO6" LISTING

```
10 REM WAKEFLO6
15 DIM Y(40),Z(40),B(40),Y1(40),U(40)
16 DIM Z1(40),D(40),Y2(40),Y3(40),H(40),R(40),M(40),T1(40)
20 LET X=.01
22 LET M=1
24 LET T=1.01
26 LET B1=.2*(M^2)*(T+1)+T-1
28 LET C=-.2*(M^2)
30 LET P=.327591
40 LET A1=.254829592#
50 LET A2=-.284496736000001#
60 LET A3=1.421413741#
70 LET A4=-1.453152027#
80 LET A5=1.061405429#
90 PRINT "COMPLETELY ASYMMETRIC (P=0) WAKE PROFILES"
100 PRINT "-----------------------------------------------------"
110 PRINT
120 PRINT "FOR X'=";X
122 PRINT "AND MACH NO.=";M
124 PRINT "TW/T0=";T
126 PRINT
130 PRINT "Y'","Y'/2SQR(X')","1-U/UE","T/TE-1","R/RE-1"
140 PRINT TAB(8),"M","T0/T0E-1"
150 PRINT
160 FOR Y=-3 TO 3 STEP .3
170 LET Z=SQR(X)+Y/(2*SQR(X))
175 IF Z<0 GOTO 192
180 LET B=1/(1+P*Z)
190 LET Y1=(A1*B+A2*(B^2)+A3*(B^3)+A4*(B^4)+A5*(B^5))*EXP(-(Z^2))
191 GOTO 200
192 LET Z=-Y/(2*SQR(X))-SQR(X)
194 LET B=1/(1+P*Z)
196 LET Y1=2-(A1*B+A2*(B^2)+A3*(B^3)+A4*(B^4)+A5*(B^5))*EXP(-(Z^2))
200 LET U=.5*EXP(X+Y)*Y1
210 LET Z1=2*SQR(X)+Y/(2*SQR(X))
220 IF Z1<0 GOTO 260
230 LET D=1/(1+P*Z1)
240 LET Y2=(A1*D+A2*(D^2)+A3*(D^3)+A4*(D^4)+A5*(D^5))*EXP(-(Z1^2))
250 GOTO 290
260 LET Z1=-Y/(2*SQR(X))-2*SQR(X)
270 LET D=1/(1+P*Z1)
280 LET Y2=2-(A1*D+A2*(D^2)+A3*(D^3)+A4*(D^4)+A5*(D^5))*EXP(-(Z1^2))
290 LET H=.5*C*EXP(4*X+2*Y)*Y2+B1*U
300 LET Y3=Y/(2*SQR(X))
310 LET R=-H/(H+1)
320 LET M1=(1-U)*M*SQR(1+R)
330 LET T1=((H+1)*(1+.2*(M1^2))/(1+.2*(M^2)))-1
350 PRINT Y,Y3,U,H,R
360 PRINT TAB(8),M1,T1
380 NEXT Y
1000 END
```

"WAKEFLOG" OUTPUT

COMPLETELY ASYMMETRIC (P=0) WAKE PROFILES

FOR X'= .01
AND MACH NO.= 1
TW/T0= 1.01

Y'	Y'/ZSQR(X')	1-U/UE	T/TE-1	R/RE-1
	M	T0/T0E-1		
-3	-15	.0502874	.0202024	-.0198024
	.940262	4.94242E-04		
-2.7	-13.5	.0478809	.0270268	-.0263155
	.919773	6.63281E-04		
-2.4	-12	.0916297	.0360383	-.0347847
	.892422	8.87871E-04		
-2.1	-10.5	.123687	.0478376	-.0456536
	.856076	1.18542E-03		
-1.8	-9	.16696	.0630998	-.0593546
	.807939	1.57571E-03		
-1.5	-7.5	.225373	.0824898	-.0762037
	.744528	2.08271E-03		
-1.2	-6	.304221	.106455	-.0962128
	.661461	2.73061E-03		
-.9	-4.5	.410656	.134781	-.118773
	.553239	3.53885E-03		
-.6	-3	.554316	.165683	-.142134
	.412798	0045085		
-.3	-1.5	.730412	.190457	-.159987
	.247084	4.16076E-03		
-2.38419E-07	-1.19209E-06	.448229	.103768	-.0940128
	.225194	-.0294513		
.3	1.5	.0161236	3.56882E-03	-3.55613E-03
	.982125	-2.35724E-03		
.6	3	1.07279E-05	2.33564E-06	-2.33563E-06
	.999988	-1.60933E-06		
.9	4.5	9.67404E-11	2.08958E-11	-2.08958E-11
	1	0		
1.2	6	1.07256E-17	2.30624E-18	-2.30624E-18
	1	0		
1.5	7.5	1.40302E-26	3.00816E-27	-3.00816E-27
	1	0		

"WAKEFL07" PROGRAM

1. Purpose: To compute completely asymmetric (P = 0) wake profiles of velocity, density, etc. normalized so that the maximum value of each profile is 1.0. This is done for a fixed x', M_e and T_w/T_o. The program requires inputs from the WAKEFL06 program in the form of the extreme (center) values of velocity, temperature and density.

2. Application Example

Compute the normalized profiles for the P = 0 wake when $x' = 0.3$, $M_e = 6$, $T_w/T_o = 0.2$ for $-3 < y' < 3$ in steps of 0.05. For this case, the WAKEFL06 program gives the following center values:

$(1 - \frac{u}{u_e})_c = 0.3705$

$(\frac{T}{T_e} - 1)_c = 1.426$

$(\frac{\rho}{\rho_e} - 1)_c = -0.5879$

Enter:

```
20  LET X = 0.3
22  LET M = 6
24  LET T = 0.2
82  LET U   = 0.3705
84  LET T   = 1.426
86  LET R   = -0.5879
160  FOR Y = -3 TO 3 STEP 0.06
```

3. Explanation of Output Symbols

Y´	y´
Y´/2SQR(x´)	F
1 - U/UE	$(u_e - u)/u_e - u_c)$
T/TE - 1	$(T - T_e)/(T_c - T_e)$
R/RE - 1	$(\rho - \rho_e)/(\rho_c - \rho_e)$

"WAKEFLO7" LISTING

```
10 REM WAKEFLO7
15 DIM Y(100),Z(100),B(100),Y1(100),U(100)
16 DIM Z1(100),D(100),Y2(100),Y3(100),H(100),R(100),M(100),T1(100)
20 LET X=.3
22 LET M=6
24 LET T=.2
26 LET B1=.2*(M^2)*(T+1)+T-1
28 LET C=-.2*(M^2)
30 LET P=.327591
40 LET A1=.254829592#
50 LET A2=-.284496736000001#
60 LET A3=1.421413741#
70 LET A4=-1.453152027#
80 LET A5=1.061405429#
82 LET U9=.3705
84 LET T9=1.426
86 LET R9=-.5879
90 PRINT "NORMALIZED PROFILES FOR COMPLETELY ASYMMETRIC (P=0) CASE"
100 PRINT "-------------------------------------------------"
110 PRINT
120 PRINT "FOR X'=";X
122 PRINT "AND MACH NO.=";M
124 PRINT "TW/T0=";T
125 PRINT "CENTER 1-U/UE IS=";U9
126 PRINT "CENTER T/TE-1=";T9
127 PRINT "CENTER R/RE-1=";R9
128 PRINT
129 PRINT
130 PRINT "Y'","Y'/2SQR(X')","(1-U/UE)*","(T/TE-1)*","(R/RE-1)*"
150 PRINT
160 FOR Y=-3 TO 3 STEP .06
170 LET Z=SQR(X)+Y/(2*SQR(X))
175 IF Z<0 GOTO 192
180 LET B=1/(1+P*Z)
190 LET Y1=(A1*B+A2*(B^2)+A3*(B^3)+A4*(B^4)+A5*(B^5))*EXP(-(Z^2))
191 GOTO 200
192 LET Z=-Y/(2*SQR(X))-SQR(X)
194 LET B=1/(1+P*Z)
196 LET Y1=2-(A1*B+A2*(B^2)+A3*(B^3)+A4*(B^4)+A5*(B^5))*EXP(-(Z^2))
200 LET U=.5*EXP(X+Y)*Y1
210 LET Z1=2*SQR(X)+Y/(2*SQR(X))
220 IF Z1<0 GOTO 260
230 LET D=1/(1+P*Z1)
240 LET Y2=(A1*D+A2*(D^2)+A3*(D^3)+A4*(D^4)+A5*(D^5))*EXP(-(Z1^2))
250 GOTO 290
260 LET Z1=-Y/(2*SQR(X))-2*SQR(X)
270 LET D=1/(1+P*Z1)
280 LET Y2=2-(A1*D+A2*(D^2)+A3*(D^3)+A4*(D^4)+A5*(D^5))*EXP(-(Z1^2))
290 LET H=.5*C*EXP(4*X+2*Y)*Y2+B1*U
300 LET Y3=Y/(2*SQR(X))
310 LET R=-H/(H+1)
320 LET M1=(1-U)*M*SQR(1+R)
330 LET T1=((H+1)*(1+.2*(M1^2))/(1+.2*(M^2)))-1
350 PRINT Y,Y3,U/U9,H/T9,R/R9
380 NEXT Y
390 PRINT
400 PRINT "* NORMALIZED WITH THE APPROPRIATE CENTER VALUE"
1000 END
```

"WAKEFL07" OUTPUT

NORMALIZED PROFILES FOR COMPLETELY ASYMMETRIC (P=0) CASE

FOR X'= .3
AND MACH NO.= 6
TW/T0= .2
CENTER 1-U/UE IS= .3705
CENTER T/TE-1= 1.426
CENTER R/RE-1=-.5879

Y'	Y'/2SQR(X')	(1-U/UE)*	(T/TE-1)*	(R/RE-1)*
-3	-2.73861	.181215	.327995	.542051
-2.94	-2.68384	.192365	.34557	.561508
-2.88	-2.62907	.204186	.363893	.581108
-2.82	-2.5743	.216714	.382967	.60081
-2.76	-2.51952	.229983	.402795	.620567
-2.7	-2.46475	.244032	.423371	.640334
-2.64	-2.40998	.258895	.444685	.660061
-2.58	-2.35521	.27461	.466722	.6797
-2.52	-2.30044	.291209	.489456	.6992
-2.46	-2.24566	.308726	.512857	.718508